ORNL/TM-6001

Creep-Rupture Properties and Corrosion Behavior of 2¼ Cr-1 Mo Steel and Hastelloy X Alloys in Simulated HTGR Environment—Interim Report

Aage S. Lystrup
P. L. Rittenhouse
J. R. DiStefano

OAK RIDGE NATIONAL LABORATORY
OPERATED BY UNION CARBIDE CORPORATION FOR THE ENERGY RESEARCH AND DEVELOPMENT ADMINISTRATION

DISCLAIMER

Printed in the United States of America. Available from
National Technical Information Service
U.S. Department of Commerce
5285 Port Royal Road, Springfield, Virginia 22161
Price: Printed Copy $4,50; Microfiche $3.00

ORNL/TM-6001
Distribution
Category UC-77

Contract No. W-7405-eng-26

METALS AND CERAMICS DIVISION

HTGR BASE TECHNOLOGY PROGRAM

Gas-Cooled Structural Materials Program (189a 01332)

CREEP-RUPTURE PROPERTIES AND CORROSION BEHAVIOR OF 2 1/4 Cr-1 Mo STEEL AND HASTELLOY X ALLOYS IN SIMULATED HTGR ENVIRONMENT — Interim Report

Aage S. Lystrup, P. L. Rittenhouse, and J. R. DiStefano

Date Published: November 1977

OAK RIDGE NATIONAL LABORATORY
Oak Ridge, Tennessee 37830
operated by
UNION CARBIDE CORPORATION
for the
DEPARTMENT OF ENERGY

THIS PAGE

WAS INTENTIONALLY

LEFT BLANK

CONTENTS

CREEP-RUPTURE PROPERTIES AND CORROSION BEHAVIOR OF 2 1/4 Cr-1 Mo STEEL AND HASTELLOY X ALLOYS IN SIMULATED HTGR ENVIRONMENT — Interim Report

Aage, S. Lystrup,* P. L. Rittenhouse, and J. R. DiStefano

ABSTRACT

Hastelloy X and 2 1/4 Cr-1 Mo steel are being considered as structural alloys for components of a High-Temperature Gas-Cooled Reactor (HTGR) system. Among other mechanical properties, the creep behavior of these materials in HTGR primary coolant helium must be established to form part of the design criteria. This report describes the simulated HTGR-helium environmental creep facilities, summarizes preliminary creep properties of 2 1/4 Cr-1 Mo steel and Hastelloy X generated in HTGR helium and compares these with data obtained by testing in air. Some corrosion characteristics of the two materials are also discussed.

INTRODUCTION

The HTGR design features a multiloop steam system; each independent primary coolant loop has its own steam generator and coolant circulator. Helium circulates downward through channels in the graphite-moderated core and transports heat to the steam generators. The steam generators are of the helically coiled once-through type that produce steam by "uphill boiling."

Two of the principal high-temperature structural materials in an HTGR are Hastelloy X and 2 1/4 Cr-1 Mo steel. Hastelloy X is being considered as a material for the high-temperature ducts that circulate helium to the steam generator and in other areas as a cover plate material in the thermal insulation system. This insulation protects the carbon steel liner, which is the system pressure boundary. The alloy 2 1/4 Cr-1 Mo steel is one of two high-temperature materials (Incoloy 800H is the other) in the steam generator system.

---

*Formerly on loan from Risö.

These alloys, as well as most other high-temperature alloys, were designed primarily for use in atmospheres with high oxygen partial pressures. Under these conditions the oxide scales that forms serve to minimize sub-scale oxidation and, in some cases, carburization as well. However, in HTGR helium, oxygen partial pressures are low, and the scales that form may not be protective. Since the alloys will be exposed to this type of environment for very long times (30–40 years), there could be considerable surface and bulk corrosion that could lead to significant changes in mechanical properties.

An adequate knowledge of creep and rupture properties is essential before load-bearing elevated-temperature structures can be safely and economically designed. Existing codes governing the design of components at elevated temperatures have been based on assessments of material behavior in air. The primary coolant of an HTGR, on the other hand, is unique in that it is helium that contains very low levels of impurities such as H_2, H_2O, CO, and CH_4. Some data have shown that material behavior in such environments can be different from that in air.[1–3] The purpose of this study is to determine the creep behavior of Hastelloy X and 2 1/4 Cr-1 Mo steel in HTGR Helium and to compare the behavior of the materials in helium with their behavior in air.

MATERIAL CHARACTERIZATION

The chemical composition, product form, heat treatment, and other characteristics of the material used in this program are shown in Table 1. Four heats of 2 1/4 Cr-1 Mo steel were isothermally annealed.

---

[1]D. S. Wood, N. Farrow, and W. T. Burke, "A Preliminary Study of the Effects of Helium Environment on the Creep and Rupture Behavior of Type 316 Stainless Steel and Incoloy 800," pp. 213–28 in *Effects of Environment on Material Properties in Nuclear Systems* (Proceedings of the International Conference on Corrosion, London, July 1–2, 1971), Institution of Civil Engineers, London, 1971.

[2]J. Board, "The Effects of a Helium Environment on the High Temperature Properties of Structural Materials," *J. Br. Nucl. Energy Soc.* 10: 101–13 (1970).

[3]P. L. Rittenhouse, *Initial Assessment of the Status of HTGR Metallic Structural Materials Technology*, ORNL-TM-4760 (December 1974).

Table 1. Material Characterization

Alloy (form)	OD mm (in.)	Thickness mm (in.)	Heat and Source	ASME Specification	Heat Treatment	Grain Size (μm)	Grain Size ASTM	Hardness (DPH)	Ni	Cr	Fe	Mo	Co	W	Mn	Si	C	P	S	B
2 1/4 Cr-1 Mo steel (tube)	51 (2.0)	8.9 (0.35)	63202 Babcock and Wilcox	SA-213, grade T22	927 ± 14°C for 30 min, cooled to 704 ± 14°C at a maximum rate of 83°C/hr, held at 704 ± 14°C for 2 hr, cooled at room temperature at a maximum rate of 6°C/min	20–27	7–8	146		2.24	Bal.	0.96			0.43	0.34	0.12	0.012	0.023	
2 1/4 Cr-1 Mo steel (tube)	51 (2.0)	8.9 (0.35)	X-6216 Babcock and Wilcox	SA-213, grade T22	Same as heat 36202	27	7	146		2.19	Bal.	1.00			0.44	0.26	0.12	0.013	0.016	
2 1/4 Cr-1 Mo steel (tube)	51 (2.0)	8.9 (0.35)	72768 Babcock and Wilcox	SA-213, grade T22	Same as heat 36202	27	7	145		2.16	Bal.	0.94			0.41	0.38	0.10	0.014	0.012	
2 1/4 Cr-1 Mo steel (plate)		25 (1)	20017 Babcock and Wilcox	SA-387, grade D	927 ± 14°C for 1 hr, cooled to 704 ± 14°C at a maximum rate of 83°C/hr, held at 704 ± 14°C for 2 hr, cooled at room temperature at a maximum rate of 6°C/min	55–80	4–5	150		2.13	Bal.	0.90			0.55	0.29	0.11	0.012	0.014	
Hastelloy X (plate)		13 (0.5)	2600-3-4936 Cabot-Stellite	SB-435	Solution annealed at 1177°C (2150°F) followed by rapid cooling	80	4	190	Bal.	21.82	19.09	9.42	1.68	0.63	0.58	0.44	0.07	0.016	<0.005	<0.002
Hastelloy X (bar)		31.8 (1 1/4)	2600-3-2792 Cabot-Stellite	SB-572	Same as heat 2600-3-4936	55	5	197	Bal.	21.25	18.96	8.99	1.94	0.56	0.57	0.41	0.10	0.18	<0.005	<0.002

(A description of this heat treatment is given later in this report under Results and Discussion — Tensile Properties, and in Table 1.) Three of the heats were used in the creep test program, and the fourth heat, 20017, was used as corrosion specimens in the simulated HTGR-helium environment.

Heat 2600-3-4936 was used for almost all of the Hastelloy X experiments. However, two creep tests were conducted with heat 2600-3-2792. All specimens of Hastelloy X tested were mill-annealed.

Pretest photomicrographs showing the microstructure of the 2 1/4 Cr-1 Mo steel and the Hastelloy X specimens are presented in Figs. 1 and 2, repsectively. Carbide precipitates appear in all the isothermally annealed 2 1/4 Cr-1 Mo steel; M_3C, $M_{23}C_6$, M_7C_3, M_6C, and M_2C_3 are among the possible precipitated carbides.[4] Solution annealed Hastelloy X shows only a few precipitate particles which, according to Jablonski,[5] are mainly M_6C and $M_{23}C_6$.

Tensile tests on both 2 1/4 Cr-1 Mo steel and Hastelloy X were conducted in the early phase of this program, and the results have been published,[6,7] and are summarized here to provide general data appropriate for characterization of the materials. The tensile properties of isothermally annealed 2 1/4 Cr-1 Mo steel in the temperature range of 20–595°C (70–1100°F) were measured on specimens with a 3.18 mm (0.125 in.) diameter and 28.6 mm (1.125 in.) gage length. The results are shown in Table 2. Both the offset yield strength and the ultimate tensile strength are consistent with the values in the *Nuclear Materials Handbook.*[8]

---

[4]C. R. Brinkman et al., *Interim Report on the Continuous Cycling Elevated Temperature Fatigue and Subcritical Crack Growth Behavior of 2 1/4 Cr-1 Mo Steel,* ORNL/TM-4933 (December 1975).

[5]D. A. Jablonski, "High Temperature Fatigue Crack Propagation Behavior of Two Super Alloys," Master's Thesis, Massachusetts Institute of Technology, January 1976.

[6]P. L. Rittenhouse, "Tensile Testing," *HTGR Base-Technology Program Prog. Rep. Jan. 1, 1974–June 30, 1975,* ORNL-5108 pp. 67–72.

[7]C. R. Brinkman et al., *Application of Hastelloy X in Gas-Cooled Reactor Systems,* ORNL/TM-5405 (October 1976).

[8]*Nuclear Systems Materials Handbook,* Vol. 1 — Design Data, TID-26666, (continually updated).

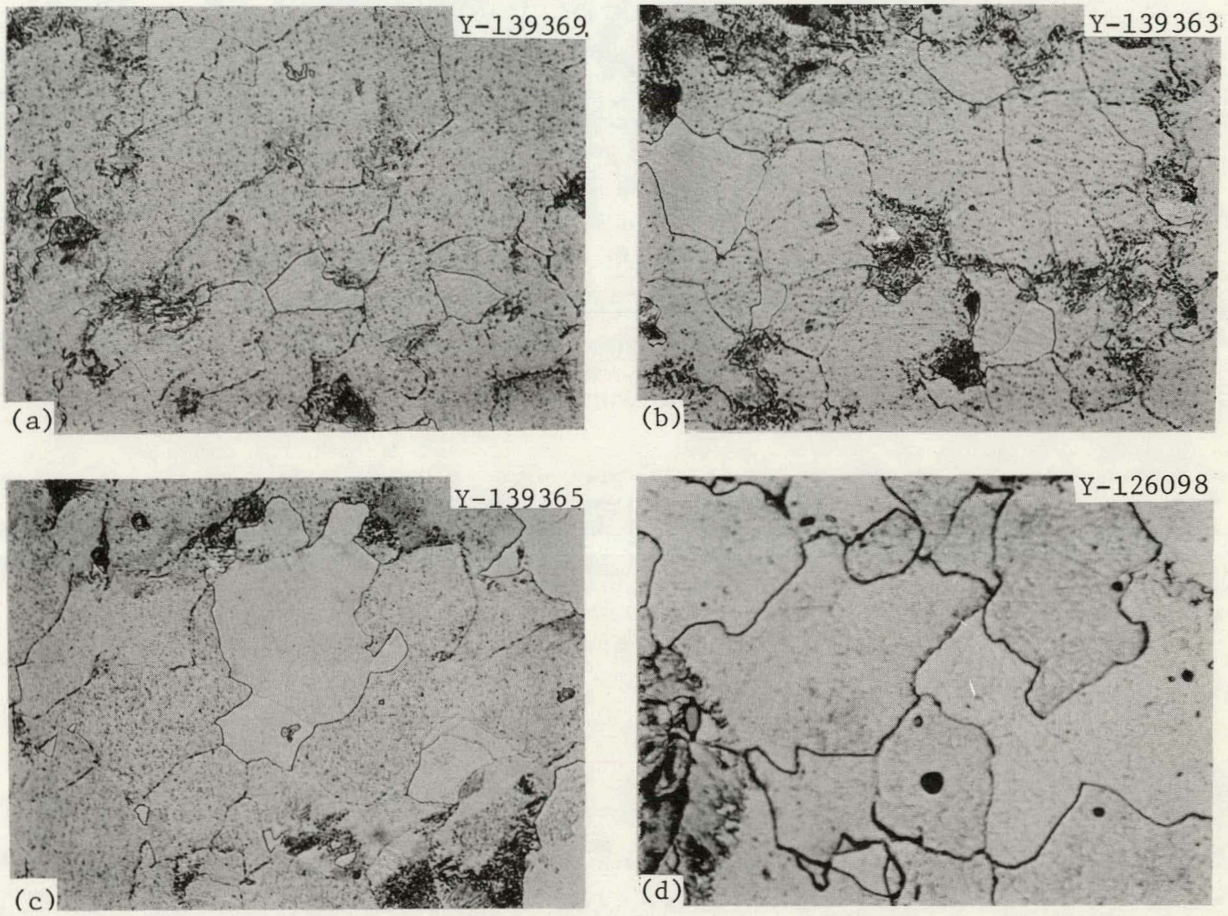

Fig. 1. Microstructure of Isothermally Annealed 2 1/4 Cr-1 Mo Steel. (a) Heat 72768. (b) Heat 36202. (c) Heat X-6216. (d) Heat 20017. 500×.

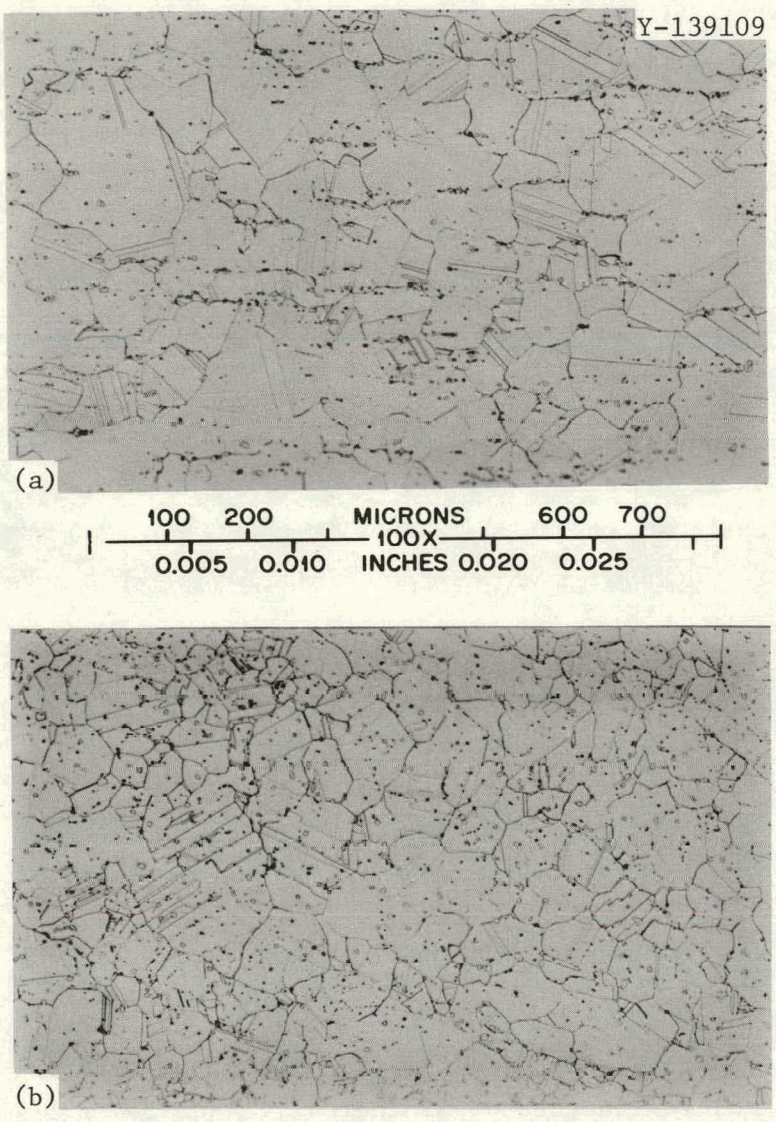

Fig. 2. Microstructure of Hastelloy X. (a) Heat 2600-3-4936. (b) Heat 2600-3-2792.

Table 2. Tensile Properties of Isothermally Annealed 2 1/4 Cr-1 Mo Steel

Test	Heat	Temperature (°C)	Temperature (°F)	Tensile Strength 0.2% Yield (MPa)	0.2% Yield (ksi)	Ultimate (MPa)	Ultimate (ksi)	Elongation in 28.6 mm (1.125 in.), % Total	Uniform	Reduction of Area (%)
14496	72768	20	70	223	32.4	476	69.0	24.6	14.9	74.8
14497	72768	20	70	221	32.1	476	69.0	26.5	15.5	77.2
14159	72768	20	70	230	33.3	452	65.5	25.5	14.9	74.1
14162	72768	20	70	236	34.2	471	68.3	24.6	14.6	73.7
14498	36202	20	70	250	36.2	507	73.5	23.2	14.1	72.5
14105	36202	20	70	257	37.3	504	73.1	23.7	14.6	71.2
14106	36202	20	70	253	36.7	502	72.8	23.3	13.4	71.1
14499	36202	20	70	225	32.7	501	72.7	25.9	14.2	72.5
14492	X-6216	20	70	244	35.4	498	72.3	2.26	13.8	73.1
14493	X-6216	20	70	241	34.9	494	71.6	23.6	14.0	69.7
14484	X-6216	20	70	241	35.0	494	71.6	23.7	14.1	70.5
14495	X-6216	20	70	240	34.8	494	71.7	24.3	14.6	73.2
14152	72768	260	500	179	25.9	388	56.3	18.7	10.8	71.6
14153	72768	260	500	178	25.8	383	55.5	19.0	11.0	74.9
14154	36202	260	500	190	27.5	416	60.3	18.7	11.0	71.1
14155	36202	260	500	195	28.3	414	60.0	17.9	10.8	70.4
14151	X-6216	260	500	197	28.6	425	61.6	17.6	10.7	73.9
14111	X-6216	260	500	194	28.1	403	58.5	18.1	10.6	73.3
14066	72768	315	600	172	25.0	394	57.1	17.8	10.4	73.8
14068	72768	315	600	154	2.24	392	56.9	17.6	9.8	73.4
14071	36202	315	600	192	27.8	423	61.3	15.7	9.4	69.3
14073	36202	315	600	190	27.6	425	61.7	18.9	10.1	68.6
14158	X-6216	315	600	186	27.0	412	59.8	15.5	8.6	68.9
14501	X-6216	315	600	190	2.75	441	64.0	15.6		68.9
14502	72768	370	700	168	23.7	428	62.1	17.1	9.6	71.5
14070	72768	370	700	182	26.4	436	63.3	17.0	11.7	70.3
14086	36202	370	700	179	25.9	445	64.6	16.5	9.9	65.3
14503	36202	370	700	179	26.0	452	65.5	16.0	10.1	66.4
14067	X-6216	370	700	181	26.3	436	63.3	17.9	10.6	66.9
14069	X-6216	370	700	188	27.2	433	62.8	15.3	9.0	69.1
14089	72768	425	800	165	23.9	399	57.9	19.7	11.8	72.5
14091	72768	425	800	143	20.7	397	57.6	19.2	11.1	71.0
14505	72768	425	800	178	25.8	408	59.2	21.3	12.6	74.0
14504	36202	425	800	170	24.7	437	63.4	19.1	10.7	67.9
14089	36202	425	800	203	29.4	427	62.0	17.5	10.5	66.3
41075	X-6216	425	800	180	26.1	415	60.2	18.6	10.5	70.6
14088	X-6216	425	800	191	27.7	391	56.7	24.7	10.4	69.9
14092	72768	480	900	162	23.5	362	52.5	22.6	11.4	78.6
14093	72768	480	900	184	26.7	362	52.5	23.1	11.9	76.8
14506	72768	480	900	157	22.7	361	52.3	26.3	11.5	81.5
14095	36202	480	900	173	25.1	390	56.6	21.9	11.1	70.0
14096	36202	480	900	184	26.7	390	56.5	21.5	10.3	82.3
14087	X-6216	480	900	161	23.3	376	54.5	20.9	10.7	74.7
14090	X-6216	480	900	176	25.5	381	55.3	21.7	11.1	76.4
14101	72768	540	1000	145	21.1	304	44.1	29.5	11.2	84.2
14104	72768	540	1000	132	19.2	305	44.2	33.0	11.1	83.1
14109	36202	540	1000	159	23.1	326	47.3	27.3	11.0	80.1
14511	36202	540	1000	168	24.4	330	47.9	29.4	10.7	78.2
14098	X-6216	540	1000	163	23.6	332	48.2	32.3	10.8	84.2
14100	X-6216	540	1000	152	22.0	318	46.1	30.8	10.6	81.6
14103	72768	595	1100	136	19.7	236	34.2	43.2	11.3	86.9
14102	72768	595	1100	116	16.8	239	34.7	41.6	10.4	87.8
14513	72768	595	1100	133	19.3	234	33.9	46.8	10.7	91.2
14512	36202	595	1100	136	19.6	254	36.8	43.8	10.5	83.5
14108	36202	595	1100	145	21.1	257	37.3	40.2	9.9	86.0
14097	X-6216	595	1100	136	19.7	250	36.2	40.8	9.9	81.4
14099	X-6216	595	1100	151	21.9	250	36.2	41.9	9.4	86.2

Specimens of Hastelloy X, Heat 2600-3-4936, were tensile-tested (Table 3) in a temperature range of 20—870°C (70—1600°F). Specimens tested measured 6.35 mm (0.25 in.) in diameter and 31.8 mm (1.25 in.) in length and showed minimum ductility in the temperature range of 480—705°C (900—1300°F) — typical of nickel-base high-temperature alloys.

Table 3. Tensile Properties of Hastelloy X Heat 2600-3-4936

Test	Temperature		Tensile Strength				Elongation in 31.8 mm (1.25 in.), %		Reduction of Area (%)
			0.2% Yield		Ultimate				
	(°C)	(°F)	(MPa)	(ksi)	(MPa)	(ksi)	Total	Uniform	
14892	20	70	359	52.0	762	110.5	50.5	43.8	59.8
14893	20	70	349	50.6	764	110.8	51.5	43.9	59.2
14894	20	70	350	50.8	764	110.8	51.9	44.3	61.4
14895	150	300	290	42.1	682	98.9	51.1	44.7	60.6
14899[a]	150	300	288	41.8	671	97.3	51.5	45.9	59.8
14896	290	550	248	36.0	662	96.0	52.8	46.2	57.9
14897	290	550	244	35.4	651	94.4	53.7	48.3	55.9
14814	290	550	245	35.5	656	95.2	54.4	49.9	55.4
14812	425	800	223	32.4	627	91.0	56.5	51.1	56.9
14813	425	800	234	34.0	629	91.2	49.8	47.3	
14809	480	900	193	28.0	623	90.4	59.0	53.6	43.6
14810	480	900	234	34.0	622	90.2	55.9	53.0	38.4
14811	480	900	219	31.8	621	90.1	58.4	53.6	48.2
14807	540	1000	239	34.6	592	85.8	49.9	46.5	40.9
14808	540	1000	221	32.1	596	86.5	48.8	43.9	31.4
14804	595	1100	220	31.9	585	84.9	53.3	47.9	40.9
14805	595	1100	223	32.4	587	85.1	53.1	47.7	41.9
14806	595	1100	232	33.7	581	84.3	51.5	47.0	43.0
14802	650	1200	214	31.1	507	73.6	39.7	39.4	35.9
14803[a]	650	1200	213	30.9	507	73.6	39.7	37.9	39.4
14799[a]	705	1300	223	32.4	425	61.6	48.5	23.0	41.7
14800	705	1300	215	31.2	452	65.5	37.3	29.9	33.6
14801[a]	705	1300	212	30.8	460	66.7	37.6	30.8	35.9
14790[a]	760	1400	215	31.2	320	46.4	73.3	6.4	66.1
14791[a]	760	1400	217	31.5	323	46.9	75.6	7.8	68.8
14796	760	1400	217	31.5	385	55.8	66.6	11.7	55.8
14798[a]	760	1400	206	29.9	381	55.2	68.1	12.0	57.0
14792[a]	815	1500	221	32.1	241	34.9	87.2	3.0	78.9
14793[a]	815	1500	232	33.7	240	34.8	72.2	3.4	74.3
14794[a]	815	1500	231	33.5	238	34.5	74.6	3.2	77.1
14795[a]	815	1500	213	30.9	241	34.9	81.2	3.2	81.4
14797	815	1500	225	32.7	288	41.7	86.0	5.8	69.6
14815[a]	870	1600	161	23.4	165	24.0	79.8	2.1	88.9
14898[a]	870	1600	163	23.6	168	24.3	84.4	2.3	88.2

[a]Constant strain rate of 0.4%/min through failure. All other tests at this rate through yielding and then increased by a factor of 4.

TEST FACILITIES

Creep Equipment

Conventional high-precision creep testing involves a load system for applying uniaxial loads with a minimum of bending stresses, an extensometer to monitor the strain that accrues with time, and a furnace and controler for maintaining the desired test temperature within narrow limits for long periods of time. Testing in a controlled environment adds substantial complexity, effort, and cost to conventional creep testing. The ten systems that have been used for environmental tests required extensive development, including design of the specimen, load train, environmental chamber, and instrumentation for extensometry. The methods and equipment for providing and monitoring the helium environment required special attention to design and development. Six frames were also built to test control specimens in air. (Construction of 18 additional environmental creep machines and 12 additional air creep frames has now been completed, and testing was initiated in March 1977.)

Creep specimens are loaded conventionally through calibrated lever arms. The load train itself is designed to minimize bending loads by using universal joints and eliminating threaded connections. This practice is also applied to the specimens (Fig. 3) by attaching them to the load train with tapered fittings clamped over each end. The environmental chamber (Fig. 4) is constructed of austenitic stainless steel pipe (enclosed in the furnace bore) with water-cooled flanges and metal bellows at each end. The bellows further facilitate alignment of the load train. U-cup seals, lightly lubricated to minimize friction, are used where the polished pull rods enter and exit the environmental chamber.

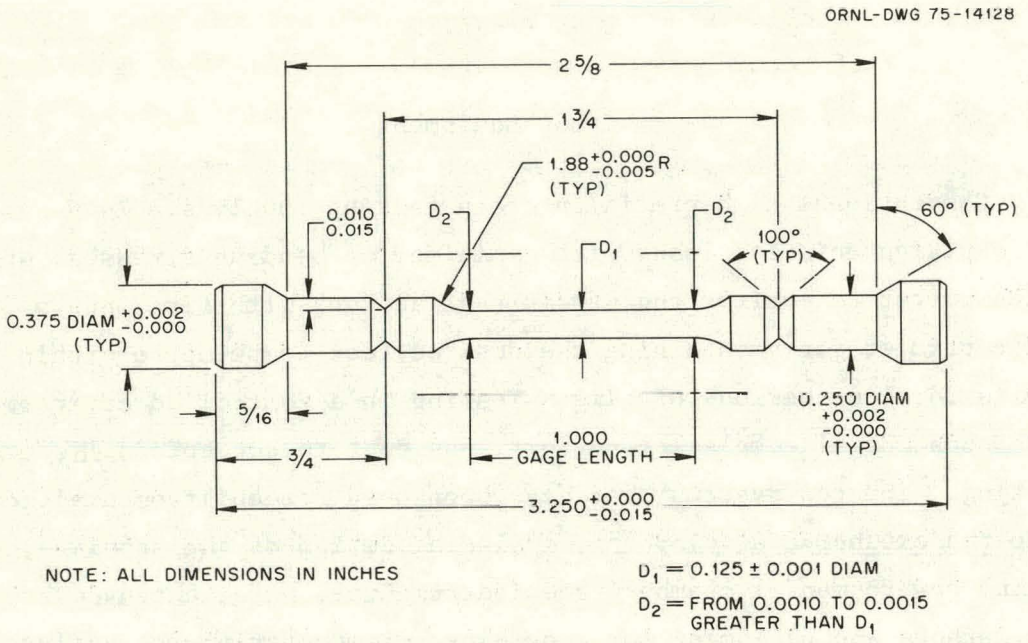

Fig. 3. Creep Test Specimen. 1 in. = 25.4 mm.

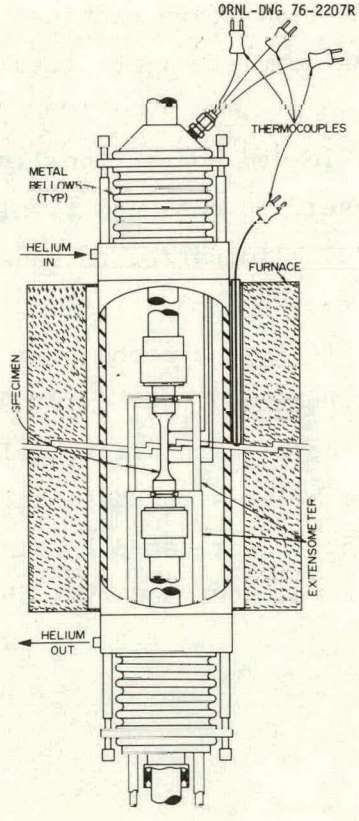

Fig. 4 Schematic of Creep Environmental Test Chamber.

This allows a positive environmental seal, yet permits application of load and unrestricted specimen extension. Seals are also used where the extensometer rods pass through the bottom of the chamber. The bores of the environmental chambers are seasoned (preoxidized) before use.

To monitor temperature, three Chromel-P—Alumel thermocouples are attached at equidistant points along the specimen gage length. The three-zone furnace surrounding the environmental chamber bore is shunted to achieve a maximum of 2°C (3.6°F) difference over the 25.4-mm (1-in.) gage length. The control thermocouple is placed in the annulus between the chamber and the furnace to avoid any possibility of reaction between the thermocouple and the helium environment that would possibly change thermocouple output. Before any test specimen is brought to temperature and loaded, the environmental chamber is evacuated and then backfilled with helium.

To measure weight gain and evaluate chemical and microstructural changes in nonstressed material exposed to HTGR helium some small corrosion specimens (Fig. 5) of both 2 1/4 Cr-1 Mo steel and Hastelloy X are being exposed to the simulated HTGR environment in the creep machines. Two corrosion specimens are mounted in the furnace with the creep specimens.

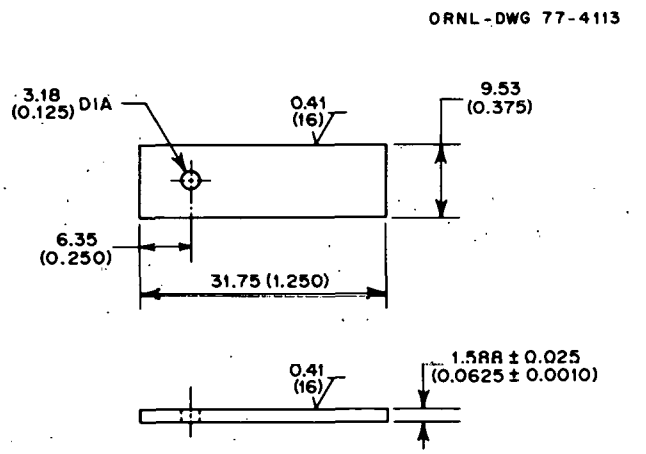

Fig. 5. Corrosion Plate Specimen.

Gas Environment System

The simulated HTGR primary coolant helium environment is supplied from premixed tanks containing controlled impurity levels of H_2, CH_4, and CO. Samples of both the entrance and exit gas from the environmental creep chambers are analyzed. The gas flow rate through each environmental creep machine is 0.17–0.25 ml/s and the pressure inside is 0.12 MPa (1.2 atm). A schematic of the premixed gas supply system is shown in Fig. 6.

The H_2, CH_4, CO, O_2, and N_2 contents of the gas are analyzed with a gas chromatograph equipped with a Micro Cross Section Detector (MCSD). Ultrapure helium (99.9999%) is used as a carrier gas. This system is very sensitive to trace impurities, but to obtain satisfactory and reproducible response the system must be leaktight.

The response of the chromatograph depends, among many other things, on the sample size injected into the column. To ensure that the same sample size is taken each time both the pressure and the volume of

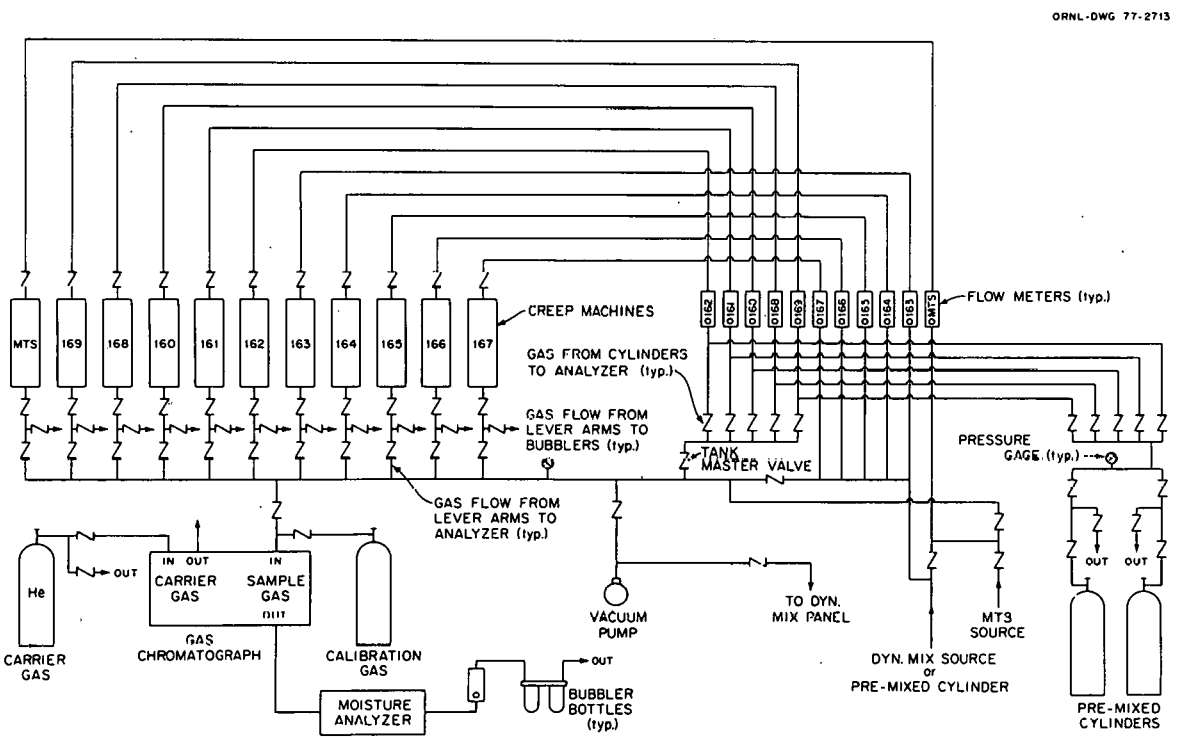

Fig. 6. Schematic of the HTGR Environmental Gas System.

the sample must be accurately controlled. A sample valve diverts a gas sample into a fixed-volume loop before injection into the chromatograph. This provides for the injection of exactly the same sample volume each time and the pressure in the sample line is kept constant. Because of the complexity of the gas (high H_2 contents and low concentrations of CH_4 and CO) sample loops containing different volumes are used to obtain accurate results. One of the sample valves introduces the gas into a loop with a large volume [3-m-long, 3.18-mm-diam tube (10 ft × 1/8 in.)] to analyze gases other than hydrogen, and a second much smaller loop is used to analyze hydrogen. A valve programmer automatically injects the large and the small volumes during a single cycle. The large sample volume is injected first, and the small one is injected when the analysis of the large one is completed. A typical chromatogram is shown in Fig. 7. To determine the concentration of each component, the area under the peak is compared with the area under the corresponding peak obtained from a gas of known composition.

Moisture is analyzed on a trace moisture analyzer that makes determinations based on simultaneous absorption and electrolysis of water.

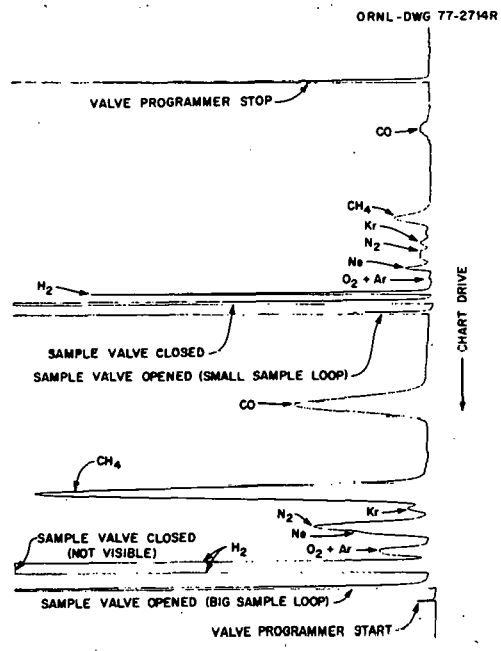

Fig. 7. Typical Gas Chromatogram Obtained from an Entrance Gas. Column: 3-m-long, 3.18-mm-diam (10 ft × 0.125 in.), molecular sieve 5A.

SIMULATED HTGR-HELIUM ENVIRONMENT

Impurity levels in the simulated HTGR primary coolant helium before entering and after leaving the environmental chambers are typified by the values given in Table 4, which also shows environmental characteristics for other test facilities and HTGRs (see Table 5 for data sources). Comparison of those gas impurity levels indicates that the ORNL test environment is relevant. Differences between the inflowing and effluent gas concentrations are due to gas-gas and metal-gas reactions occurring within the system. The HTGR helium is generally a reducing gas mixture, and the oxygen concentration is determined by equilibrium reactions among the species present in the hot furnace. The oxygen content of the entrance gas measured by the gas chromatograph is not the oxygen level to which the creep specimen is exposed. Among others, the two following reactions will occur:

$$H_2 + 1/2\ O_2 \rightleftharpoons H_2O\ ,$$

$$CO + 1/2\ O_2 \rightleftharpoons CO_2\ .$$

The first reaction is dominant,[9] and the partial pressure of oxygen is mainly determined by

$$P_{O_2} = (P_{H_2O}/KP_{H_2}\ ,$$

where K is the equilibrium constant. A typical value of the ratio P_{H_2O}/P_{H_2} in an exit gas is 0.073, and at 750°C the equilibrium constant $K = 5.75 \times 10^9$, which gives an oxygen partial pressure of 1.6×10^{-17} Pa (1.6×10^{-22} atm) if equilibrium is reached. This low value cannot be detected on the gas chromatograph, but a chromatogram of an exit gas generally shows a reverse reposnse to oxygen, which means that the exit

---

[9] R. J. Pearce and R. K. Wild, *Oxygen Partial Pressures in Helium Cooled Reactors and in Experimental Helium Loops*, Central Electricity Generating Board, RD/B/R2059-RPC/CM/P (71) 67 (August 1971).

Table 4. Impurity Levels in Primary Coolant HTGR Environment

Facility	Condition	Impurity Partial Pressure, μatm[b]							Pressure	
		H_2	CH_4	CO	CO_2	H_2O	O_2 + Ar[c]	N_2	(MPa)	(atm)
					Test Facilities					
ORNL	Entrance gas	275–300	30–35	15–25		4–9	1–5	4–7	0.12	1.2
	Exit gas	250–280	25–35	10–20		15–25	<1	4–15	0.12	1.2
GA		1500	50	500		50				
CIIR (Oslo)	Wet	400		400		90			0.18	1.8
	Dry	100		100		20			0.18	1.8
	Ultradry	50–100	3–8	25–50		0.5–3	d	≤11	0.18	1.8
FIAT (Italy)	Normal	200	20	40		1.5			0.18	1.8
					Reactors					
Peach Bottom	Core 1		11–34	11–34	<11		23–68	23–160	2.31	22.8
	Core 2	114–456	11–34	11–23	<11		<2	11–68	2.31	22.8
Fort St. Vrain	2% Power		20	<3	59	2350		1370	3.31	32.7
	11.4% Power	1630	122	92	109	884	211	255	3.44	34.0
	20.5% Power	3830	237	178	395	3240	213	316	4.00	39.5
	26.0% Power	1690	165	220	388	1600	236	295	4.28	42.2
Dragon (England)	Normal	10	1	8	0.4	1		12	2.03	20.0
	During H_2O injection experiment	160–220	16	160–240	34–40	16–22		2–3	2.03	20.0
AVR (Germany)	Normal	445–510	2–5	1700–1900	5	1			0.94	9.3

[a] See Table 5 for Data sources.

[b] Parts per million times total pressure in atmospheres. 1 atm = 0.10132 Pa.

[c] Oxygen and argon are normally not chromatographically separated.

[d] Below detection limit.

Table 5. Sources of Data in Table 4

Facility	Source
GA	R. J. Wolwowicz, *Creep Rupture Properties of Incoloy 800H, 2 1/4 Cr-1 Mo Steel and Hastelloy X Alloys in Simulated HTGR Environment, Interim Report*, GA-A-13876 (June 1976).
CIIR (Oslo)	H.G.A. Bates et al., "The Behavior of Metals in High Temperature Reactor Helium for Steam Generators," *Nucl. Technol.* 28(3): 427 (March 1976).
	R. J. Pearce, R.A.V. Huddle and P. Kofstadt, *Fundamental Aspects of the Interaction of the HTGR Helium with Metals and Alloys*, Central Electricity Generating Board, RD/B/R2866-RPC/CM/P(74)4-DPTN/522 (modified) (January 1974).
FIAT (Italy	H.G.A. Bates and R. H. Cook, *The Program for Environmental Creep Testing of Primary Circuit Materials at CRL, FIAT*, Dragon Project Report 933 (May 1975).
Peach Bottom	W. J. Scheffel, N. L. Baldwin, and R. W. Tomlin, *Operating History Report for the Peach Bottom HTGR*, GA-A-13907, Vol. I (August 1976).
Fort St. Vrain	*Public Service Company of Colorado 330 MW(e) High-Temperature Gas-Cooled Reactor Research and Development Program*, GA-A-13997 (October 1976).
Dragon (England) and AVR (Germany)	M. R. Everett, *Helium Impurity Levels for Compatibility Testing of HTGR Primary Circuit Materials*, Dragon Project Report 932 (May 1975).

gas contains less oxygen than the carrier gas[10] (99.9999% He). This means that oxygen present in the gas entering the test chambers reacts almost completely with H_2 and CO so that O_2 is below the limit of detection in the exit gas.

RESULTS AND DISCUSSION

Tensile Properties

Tensile tests were conducted on both 2 1/4 Cr-1 Mo steel and Hastelloy X (from room temperature through appropriate elevated temperatures) in known heat treatment conditions. The results of these tests are described below.

Tests at room temperature and at 210 to 593°C (500—1100°F) in increments of 55.5°C (100°F) were conducted on three heats (Babcock and Wilcox heats 36202, 72768, and X-6216) of 2 1/4 Cr-1 Mo steel tubing. These heats, which were also tested in our environmental creep program, were isothermally annealed [i.e., austenitized at 927°C (1700°F), held for 2 hr at 704°C (1300°F), and cooled at controlled rates from 927 to 704°C (1700—1300°F) and from 704°C (1300°F) to room temperature] before tensile testing. The 0.2% offset yield strengths and ultimate tensile strengths determined for these heats are shown in Table 2. Yield strength values tend to follow the trend of the "expected minimum yield strength vs temperature" curve given in Code Case 1592, but a number of our experimentally determined values fall somewhat below the subject curve. These values are, however, consistent with minimum yield strengths recently incorporated into the *Nuclear Systems Materials Handbook.*[11] Ultimate tensile strengths, with an intermediate temperature maximum at about 371°C (700°F), are also consistent with Handbook data.

---

[10] R. C. Cavenah, Beckman Instruments, Inc., Fullerton, Calif. W. A. Hilchey, Le Fleur Corporation, Gardena, Calif., *A Sensitive System for Analyzing Permanent Cases,* unpublished manuscript.

[11] *Nuclear Systems Materials Handbook,* Vol. 1 — Design Data, TID-26666, (continually updated).

Results of the tests on 13-mm (1/2-in.) plate Hastelloy X (Cabot Corp. Heat 2600-3-4936) are shown in Table 3. Some of the tests on Hastelloy X (see notation in Table 3) were run at a rate of 0.4%/min through failure. However, most of the tests were run at 0.4%/min through yielding and then at 1.6%/min to failure. The only property that seemed to be significantly affected by this difference in test method was reduction of area [e.g., at 760°C (1400°F), reduction of area was <60% for the two-stage rate and >79% for the other].

Creep and Creep-Rupture Behavior of 2 1/4 Cr-1 Mo Steel

We have completed 18 creep tests on isothermally annealed 2 1/4 Cr-1 Mo steel in simulated HTGR primary coolant helium environment and air, and Table 6 shows the results together with the available data from tests currently in progress.

The rupture life, time to tertiary creep, and minimum creep rate for the HTGR helium tests are compared with data from literature on air tests in Figs. 8, 9, and 10, respectively. In all three figures, the solid lines represent average values for air data and the points are taken from the HTGR environment test data. The lines are calculated from equations reported by M. K. Booker et al.[12] and fit the average of many air tests conducted at various laboratories.

In the stress-rupture plot, data points from tests conducted at General Atomic[13] are also included. It appears that there is no significant difference between the data from the helium environmental tests and air tests at the temperature-stress-time (maximum 15,200 hr) combinations tested thus far, except for the three 482°C (900°F) tests conducted at General Atomic. Those tests had rupture lives much longer than those shown by the average air tests.

---

[12]M. K. Booker, T. L. Hebble, D. O. Hobson, and C. R. Brinkman, *Mechanical Properties Correlations for 2 1/4 Cr-1 Mo Steel in Support of Nuclear Reactor Systems Design*, ORNL/TM-5329 (June 1976).

[13]R. J. Wolwowicz, *Creep Rupture Properties of Incoloy 800H, 2 1/4 Cr-1 Mo Steel and Hastelloy X Alloys in Simulated HTGR Environment, Interim Report*, GA-A-13876 (June 1976).

Table 6. Results of Creep Tests on 2 1/4 Cr-1 Mo Steels

Test	Heat	Temperature		Stress		Environment	Time to Indicated Creep Strain (hr)			Minimum Creep Rate (hr^{-1})	Time to Tertiary Creep (hr)	Rupture Life (hr)	Elongation (%)
		(°C)	(°F)	(MPa)	(ksi)		1%	2%	5%				
17495	72768	649	1200	69	10	HTGR-He	28	59	137	3.1×10^{-4}	100	288	47.2
17948	36202	649	1200	69	10	HTGR-He	47	97	204	1.8	115	361	34.6
17864	X-6216	649	1200	69	10	HTGR-He	167	248	370	0.39	140	513	29.1
18075	72768	649	1200	34	5	HTGR-He						In Progress	
17333	X-6216	593	1100	138	20	HTGR-He	5	11	34	13	42	89.5	42.1
16882	72768	593	1100	103	15	HTGR-He	0.8	3	81	0.44	600	1337	51.3
17377	72768	593	1100	103	15	HTGR-He	13	30	92	4.9	130	328	50.8
16883	36202	593	1100	103	15	HTGR-He	17	48	144	3.1	188	436	46.8
17334	X-6216	593	1100	103	15	HTGR-He	39	105	306	1.4	365	793	44.5
16266	72768	593	1100	103	15	Air	10	26	90	4.8	175	388	52.5
15023	X-6216	593	1100	69	10	HTGR-He	3186	4930	7380	0.024	3750	9660	38.9
15047	X-6216	593	1100	69	10	HTGR-He	3132	4660	6540	0.025	3150	7784	26.6
15045	X-6216	593	1100	69	10	HTGR-He				0.022		3186[b]	2.8[b]
16360	72768	593	1100	69	10	Air	971	2115	4435	0.054	1004	6698	27.3
17376	X-6216	593	1100	69	10	Air						In Progress	
13149	36202	538	1000	138	20	HTGR-He						In Progress	
17918	X-6216	538	1000	138	20	HTGR-He	75	225	674	0.67	1050	In Progress	
15369	36202	538	1000	103	15	HTGR-He	842	2047	6144	0.072	6800	15232	41.7
15046	X-6216	538	1000	103	15	HTGR-He	1122	2850	7660	0.059	8100	14957	38.2
16264	36202	538	1000	103	15	Air	1050	2700				In Progress	
17947	72768	482	900	207	30	HTGR-He	186	402	860	0.44	476	In Progress	
15373	36202	482	900	207	30	HTGR-He	349	787	1660	0.11	500	3494	35.7
17494	X-6216	482	900	207	30	HTGR-He	215	685	1885	0.22	1650	In Progress	
16263	36202	482	900	207	30	Air	204	620	1800	0.25	2030	6611	45.3
15374	36202	482	900	172	25	HTGR-He	1500	2705	5200	0.039	1300	13509	40.2
17849	36202	482	900	172	25	Air	1073					In Progress	

[a] Helium with impurities: 275 µatm H_2, 30 µatm CH_4, 20 µatm CO, 20 µatm H_2O (1 µatm = 0.101 Pa).

[b] Terminated short of rupture.

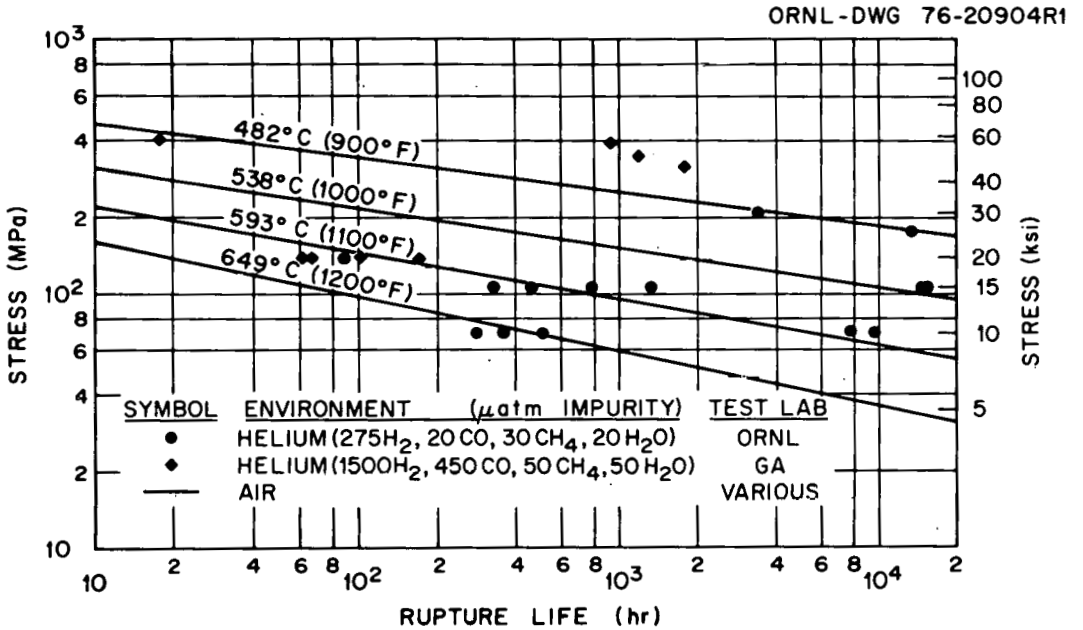

Fig. 8. Rupture Life Versus Stress for 2 1/4 Cr-1 Mo Steel in Simulated HTGR-Helium Environment and Air at Different Temperatures.

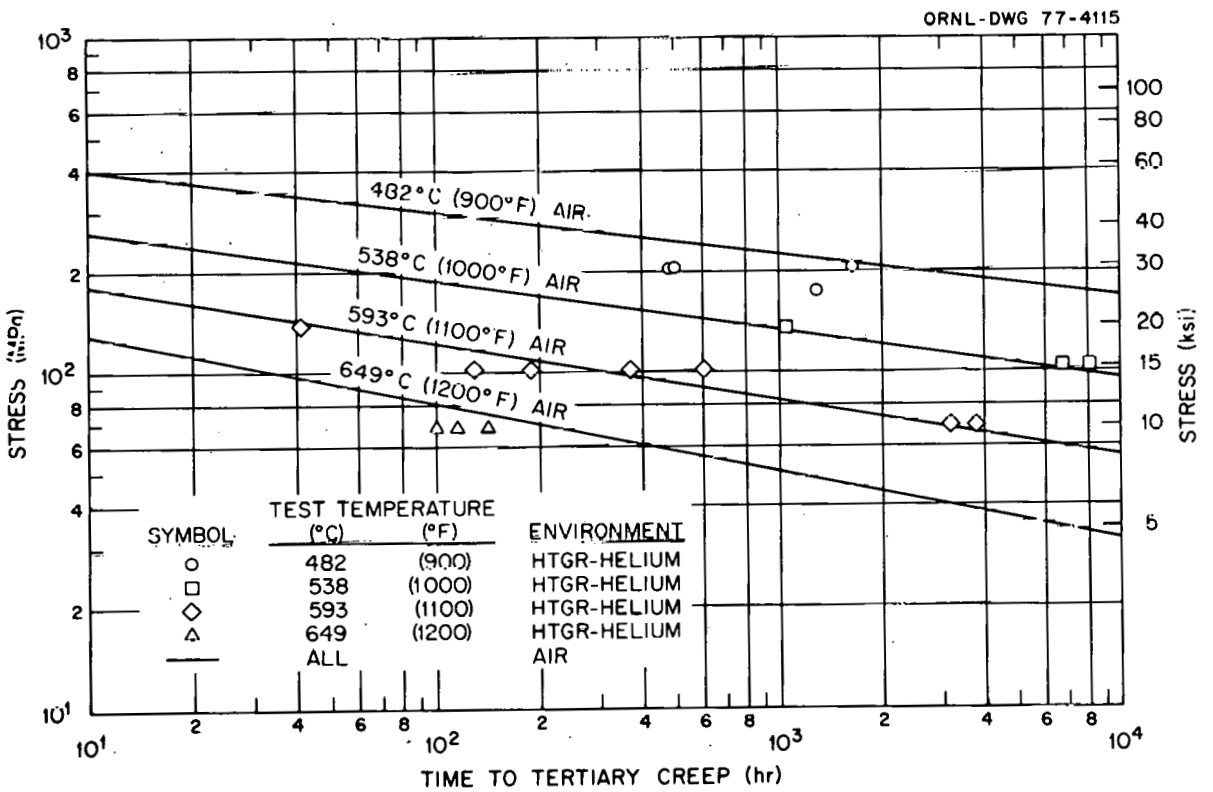

Fig. 9. Time to Tertiary Creep Versus Stress for 2 1/4 Cr-1 Mo Steel in Simulated HTGR-Helium Environment and Air at Different Temperatures.

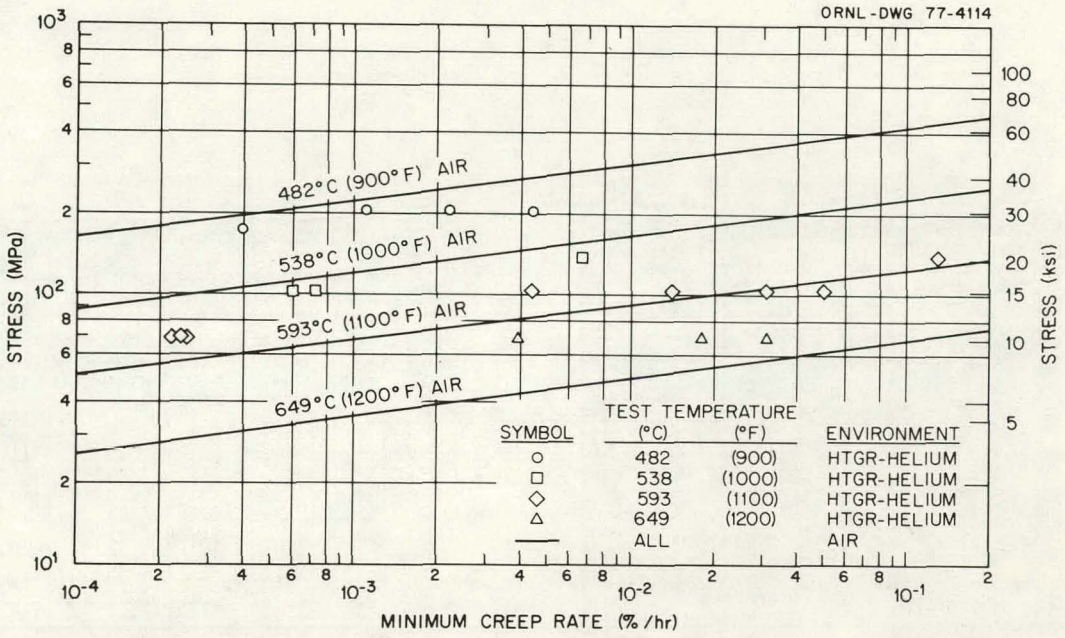

Fig. 10. Minimum Creep Rate Versus Stress for 2 1/4 Cr-1 Mo Steel in HTGR-Environment and Air at Different Temperatures.

Also, no significant differences in the times to onset of tertiary creep for the air tests and the HTGR-helium tests were observed. Actually, the pattern of the stress vs time-to-tertiary creep plot looks very similar to that of the stress-rupture plot, except at 482°C (900°F), where the tertiary creep stage started slightly earlier for the HTGR-helium tests than for the air tests.

Figure 10 is a plot of minimum creep rate vs stress. It is clear that at 649°C (1200°F) the minimum creep rate was lower for the HTGR-helium tests than for the air tests. However, it is interesting that in helium, the time to tertiary creep and the rupture life were shorter, although the differences were small.

Three tests of 2 1/4 Cr-1 Mo steel in air have been completed. In Fig. 11, their creep curves are compared with creep curves from tests conducted in the simulated HTGR-helium environment. Again, time to tertiary creep was much longer in air than in HTGR helium at 482°C (900°F) and 207 MPa (30 ksi), although the minimum creep rate was the same. At 593°C (1100°F) and 69 MPa (10 ksi), this trend was reversed and the minimum creep rate in air was twice as high as in

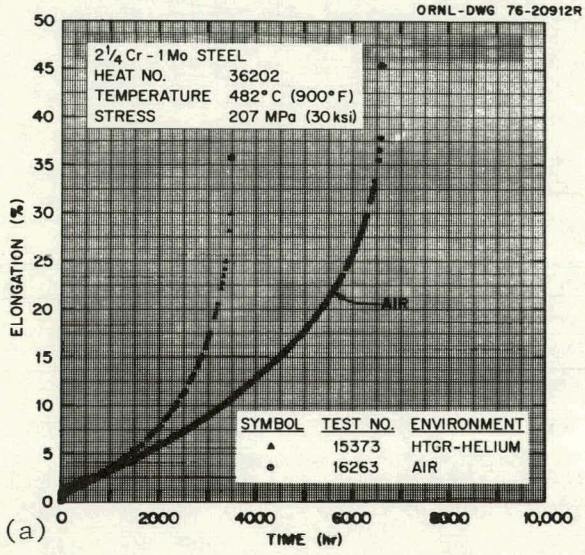

(a)

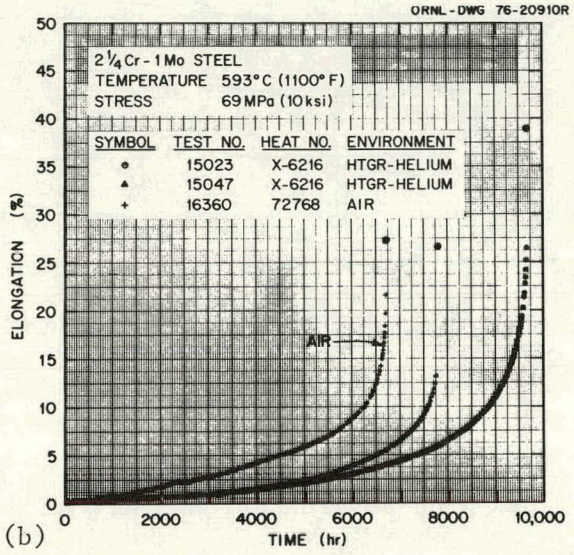

(b)

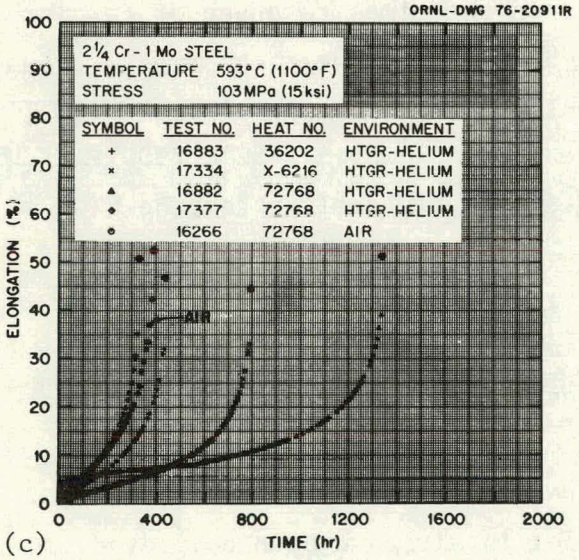

(c)

Fig. 11. Comparison of Creep Curves for 2 1/4 Cr-1 Mo Steel Conducted in Simulated HTGR-Helium Environment and Air at Three Different Test Conditions.

HTGR helium. At 593°C (1100°F) and 103 MPa (15 ksi), the creep curve for an air test was similar to two creep curves for HTGR-helium tests, whereas two other tests conducted in HTGR helium had a lower minimum creep rate and a longer time to rupture. Test 16882 showed quite different behavior. The minimum creep rate was one-tenth that for Test 17377, which was identical in all respects: same heat, same environment, and even the same creep frame.

Creep and Creep-Rupture Behavior of Hastelloy X

Fifteen creep tests of Hastelloy X have been conducted in either the simulated HTGR primary coolant helium environment or air. The results are shown in Table 7 together with the available data from additional tests that are in progress.

The rupture life, time to tertiary creep, and minimum creep rate of Hastelloy X exposed to HTGR helium are plotted as functions of stress in Figs. 12, 13, and 14, respectively. The solid lines in Figs. 12 and 14 represent data from air tests[14] included for comparison. In all these figures the points plotted are data from the HTGR environmental tests, and the dotted lines are based on those points and engineering judgment.

In the stress-rupture plot (Fig. 12) data points from tests conducted at General Atomic[15] are included, and as for 2 1/4 Cr-1 Mo steel, there is no significant difference between the rupture life of Hastelloy X in HTGR-helium and in air at these temperature-stress-time combinations (maximum time, 6500 hr). The minimum creep rate of Hastelloy X (Fig. 14) was lower in HTGR helium than in air in the temperature range 649–871°C (1200–1600°F), and the lower the stress the bigger the difference between the HTGR-helium data and air data. Although the smaller minimum

---

[14]J. W. Tackett, *The Creep Rupture Properties of Hastelloy Alloy X Sheet*, Tech. Dept. Report 8745, Stellite Division, Cabot Corporation, Kokomo, Indiana, 1975.

[15]R. J. Wolwowicz, *Creep Rupture Properties of Incoloy 800H, 2 1/4 Cr-1 Mo Steel and Hastelloy X Alloys in Simulated HTGR Environment, Interim Report*, GA-A-13876 (June 1976).

Table 7. Results of Creep Tests on Hastelloy X

Test	Heat	Temperature (°C)	Temperature (°F)	Stress (MPa)	Stress (ksi)	Environment	Time to Indicated Creep Strain, hr (1%)	(2%)	(5%)	Minimum Creep Rate (hr^{-1})	Time to Tertiary Creep (hr)	Rupture Life (hr)	Elongation (%)
16054	2600-3-2792	871	1600	62	9	HTGR-He[a]	93	197	327	0.93 × 10^{-1}	205	554	34.8
16126	2600-3-4936	871	1600	34	5	HTGR-He	1414	4000	5400	0.010	2350	6527	14.2
17850	2600-3-4936	871	1600	34	5	Air	1022						In Progress
17332	2600-3-4936	816	1500	69	10	HTGR-He	253	387[b]	1745[b]	0.14	900[b]	2790	25.8
16269	2600-3-4936	816	1500	69	10	Air	600[b]	940[b]	1720[b]	0.1[b]	650[b]	3453	18.8
17375	2600-3-4936	816	1500	69	10	Air	119	400	970	0.34	690	1905	43.7
16031	2600-3-2792	760	1400	152	22	HTGR-He	7	15	38	12.0	44	159	57.5
16125	2600-3-4936	760	1400	138	20	HTGR-He	16	30	103	4.0	142	305	38.9
17330	2600-3-4936	760	1400	138	20	Air	18	35	95	4.6	113	297	52.4
16490	2600-3-4936	760	1400	103	15	HTGR-He	377	1110	2180	0.12	1480	2690	18.7
17875	2600-3-4936	760	1400	69	10	HTGR-He							In Progress
15771	2600-3-4936	704	1300	172	25	HTGR-He	49	104	321	1.4	510	1007	35.4
15058	2600-3-4936	704	1300	138	20	HTGR-He	113	344	1920	0.17	1950	4045	21.4
15792	2600-3-4936	704	1300	138	20	HTGR-He	148	500	2590	0.11	2000	4588	23.0
16268	2600-3-4936	704	1300	138	20	Air	98	297	2139	0.12	1950	4504	18.3
17328	2600-3-4936	704	1300	103	15	HTGR-He	550						In Progress
17376	2600-3-4936	704	1300	103	15	Air	96	423					In Progress
17863	2600-3-4936	649	1200	207	30	HTGR-He	291	560	1786	0.21[c]			In Progress
15772	2600-3-4936	649	1200	172	25	HTGR-He	471	850	2170	0.17	3950	6466	34.9
16267	2600-3-4936	649	1200	172	25	Air	335	946	4512	0.048	8750		In Progress
17329	2600-3-4936	649	1200	138	20	HTGR-He	805	3163				4795	2.3[d]
13150	2600-3-4936	649	1200	133	10	HTGR-He							In Progress

[a] Helium with impurities: 275 μatm H_2, 30 μatm CH_4, 20 μatm CO, 20 μatm H_2O (1 μatm = 0.101 Pa).

[b] Estimated value. Bad extensometer readings through the whole test.

[c] Test still in minimum creep rate stage, and therefore the value is interim.

[d] Terminated short of rupture. Leak in chamber.

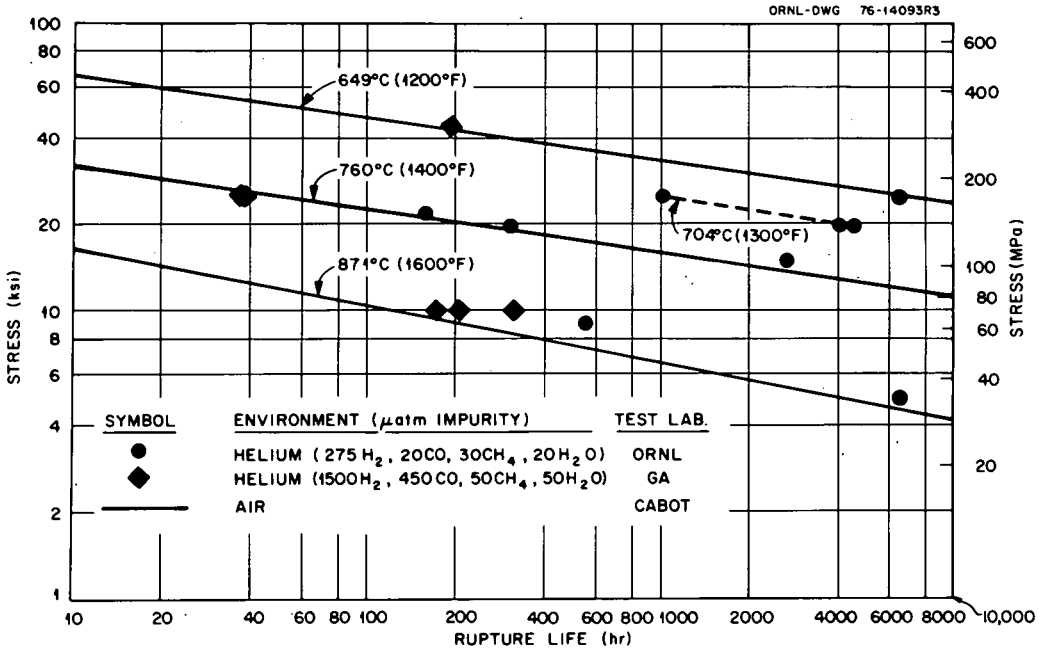

Fig. 12. Rupture Life Versus Stress for Hastelloy X in Simulated HTGR-Helium Environment and Air.

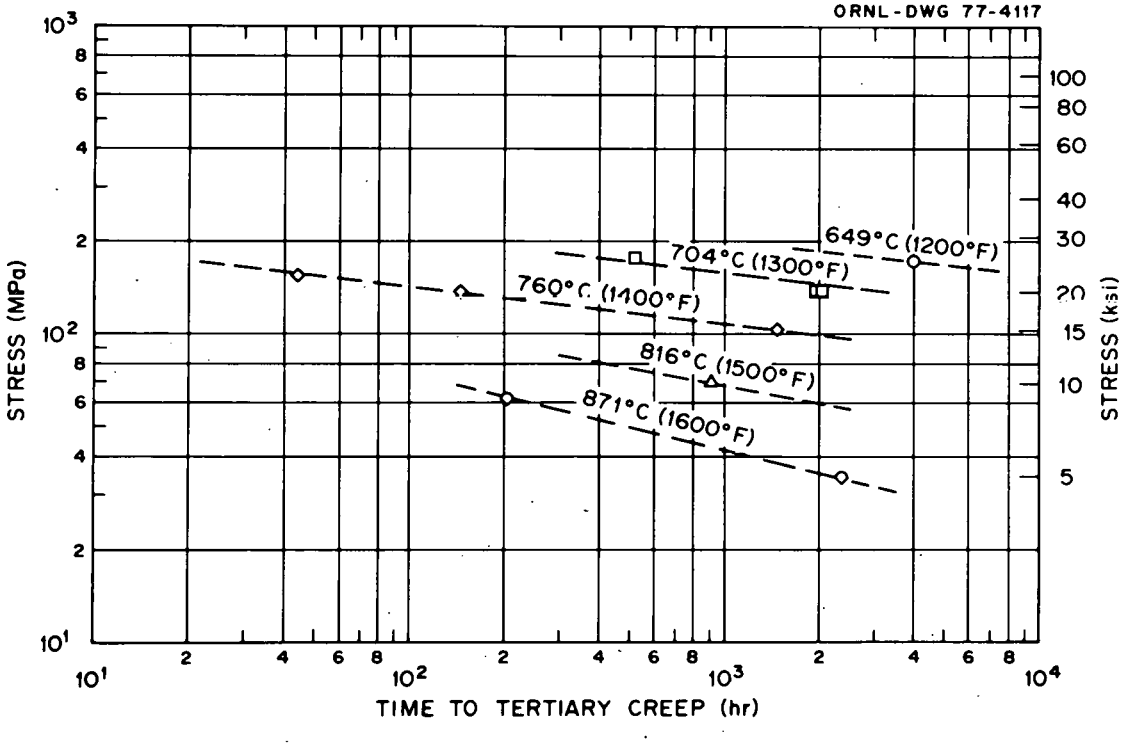

Fig. 13. Time to Teriary Creep Versus Stress for Hastelloy X in Simulated HTGR-Helium Environment.

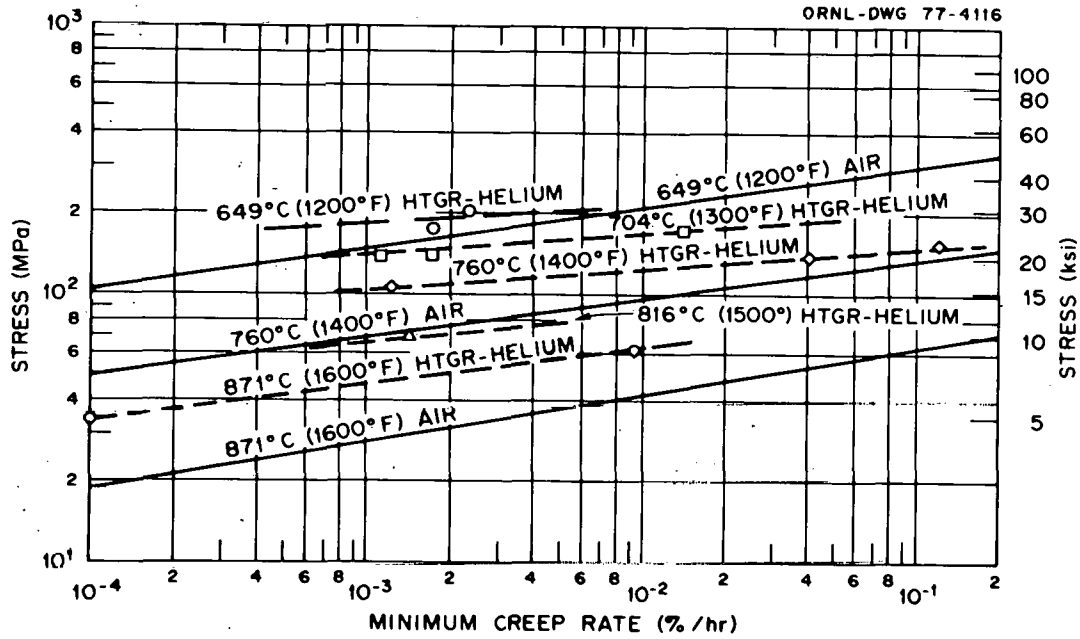

Fig. 14. Minimum Creep Rate Versus Stress for Hastelloy X in Simulated HTGR-Helium Environment and Air.

creep rate is distinct, no significantly longer rupture life in HTGR helium has been observed yet, but the data indicate that this can be expected only in very long-time tests.

Creep curves of Hastelloy X obtained in air and HTGR helium under three different tests conditions are compared in Fig. 15. There was no difference between tests conducted in air or in HTGR helium as long as the test temperature was 760°C (1400°F) or below. At 816°C (1500°F), however, the minimum creep rate was more than twice as high for the air test as for the HTGR-helium test.

Corrosion of 2 1/4 Cr-1 Mo Steel Exposed to HTGR Helium

After rupture we examined metallographically cross sections of the gage section and the shoulder of the specimens, where the stress was one-fourth that at the gage section. At 593°C (1100°F) the corrosion rate of 2 1/4 Cr-1 Mo steel decreased with increasing time. This is shown by the curve in Fig. 16, together with micrographs of the edges of cross sections of specimens from different tests. When the results are compared, the corrosion resistance of 2 1/4 Cr-1 Mo steel at

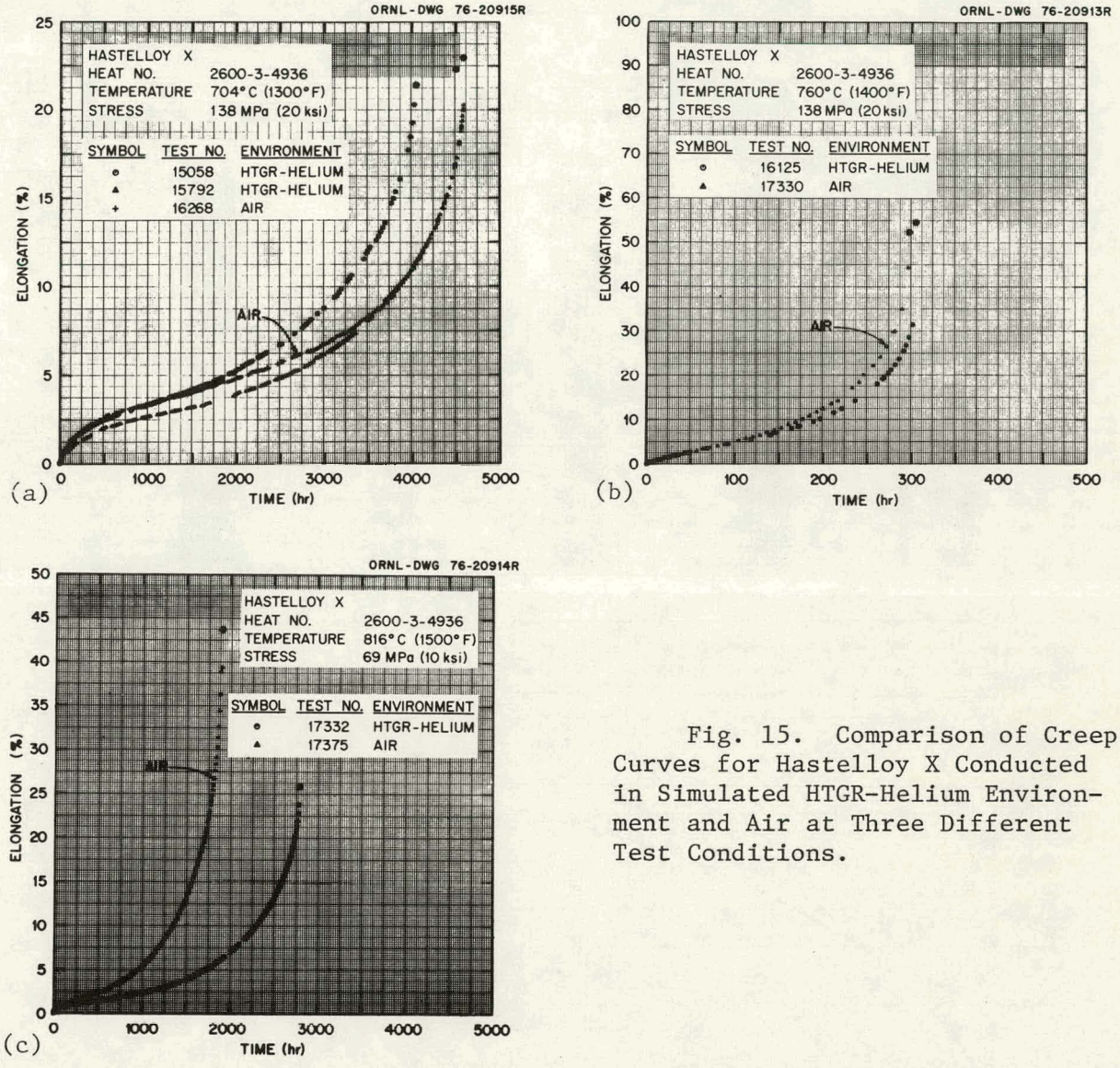

Fig. 15. Comparison of Creep Curves for Hastelloy X Conducted in Simulated HTGR-Helium Environment and Air at Three Different Test Conditions.

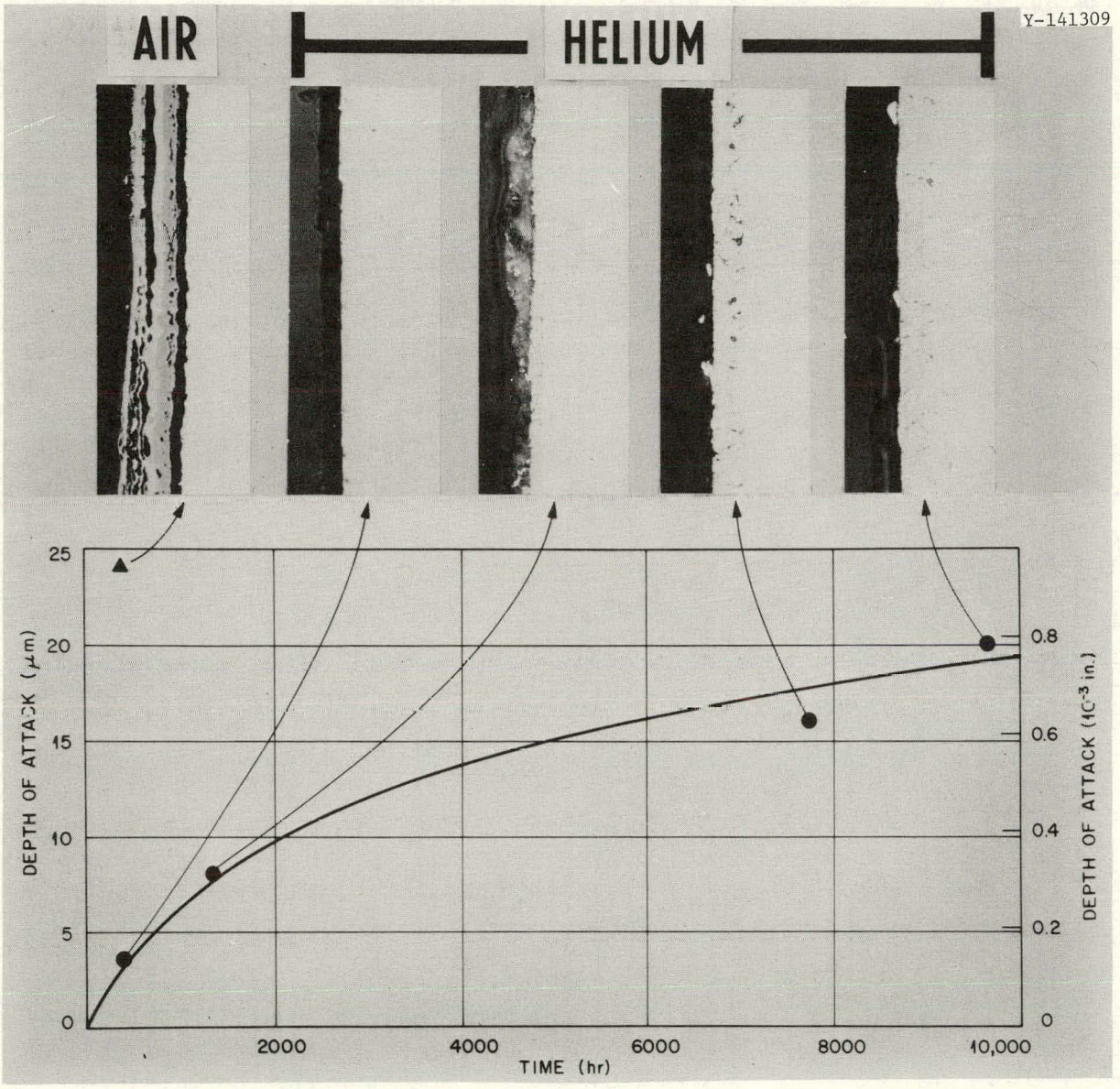

Fig. 16. Corrosion Behavior of 2 1/4 Cr-1 Mo Steel at 593°C (1100°F) in Simulated HTGR-Helium Environment and Air. The micrographs are from the following tests (left to right): 16266, 16883, 16882, 15047, and 15023.

593°C (1100°F) appears much better in HTGR helium than in air. The depth of attack in air reached 24 μm in 388 hr and 200 μm in 6698 hr (the latter result is from Test 16360 and is not shown in Fig. 16), whereas it only reached 20 μm in 9660 hr in the HTGR-helium environment. At 482°C (900°F) the amounts of attack on an air-exposed and an HTGR-helium-exposed specimen differed, but less than at 593°C (1100°F). Figure 17 shows that the oxide layer grew to a thickness of 40—50 μm after 6611 hr in air at 482°C (900°F), compared with only 6—8 μm after 13509 hr of HTGR-helium exposure.

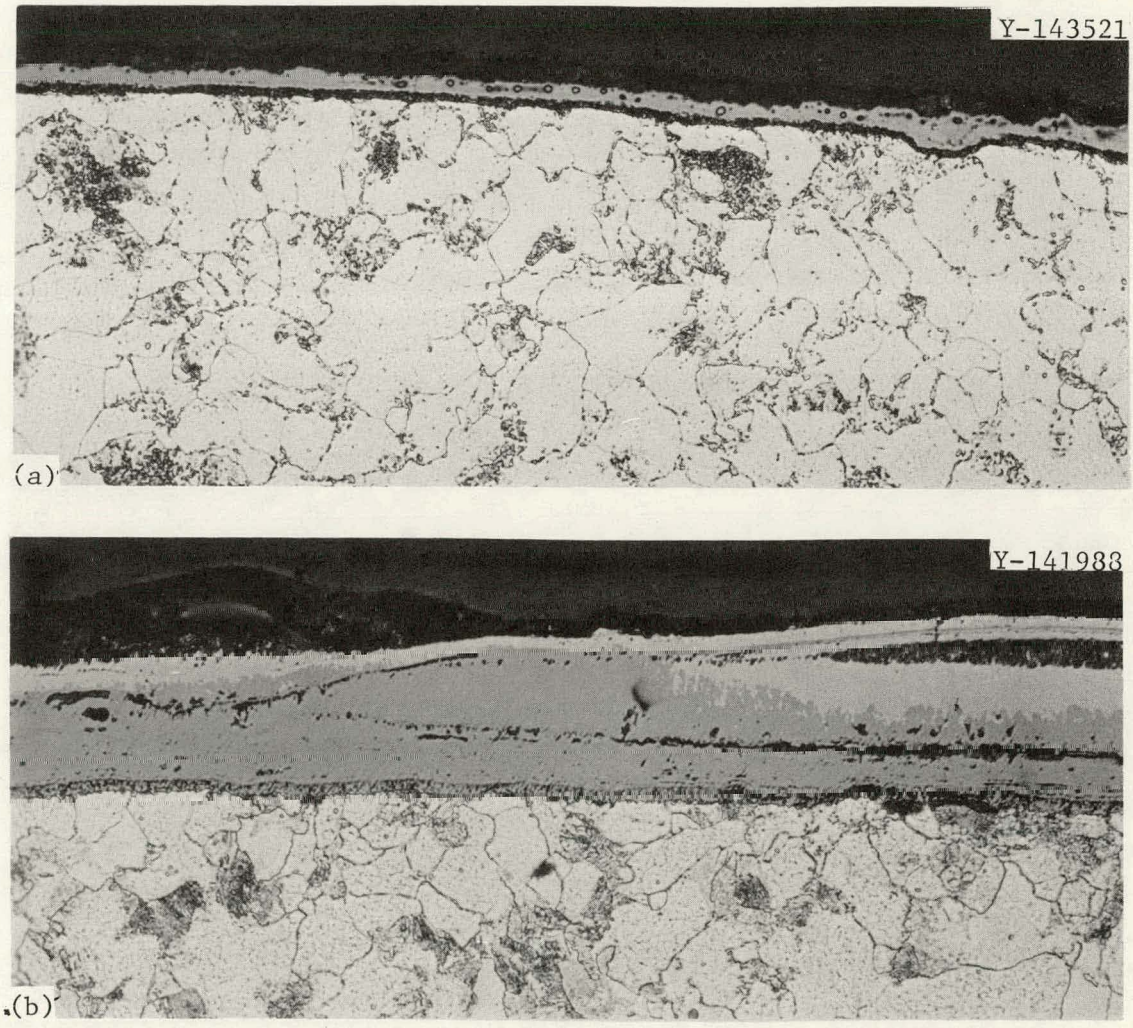

Fig. 17. Edge of Cross Section of Shoulder of 2 1/4 Cr-1 Mo Steel Specimens (Heat 36202). (a) Test 15374, HTGR-helium exposed for 13,509 hr at 482°C (900°F). (b) Test 16263, air exposed for 6611 hr at 482°C (900°F). 500×.

The three micrographs in Fig. 18 show the corrosion attack in HTGR helium as a function of temperature. The micrographs were taken of the edge of a cross section of the gage section of three specimens exposed at different temperatures, 482, 538, and 593°C (900, 1000, and 1100°F), for approximately the same time. The depth of attack obviously increases with increasing temperature. A surface oxide layer formed at all temperatures. At 482°C (900°F) the amount of intergranular attack below the oxide layer is very slight, at 538°C (1000°F) all subsurface reactions are intergranular, and at 593°C (1100°F) both intergranular and transgranular corrosion has occurred.

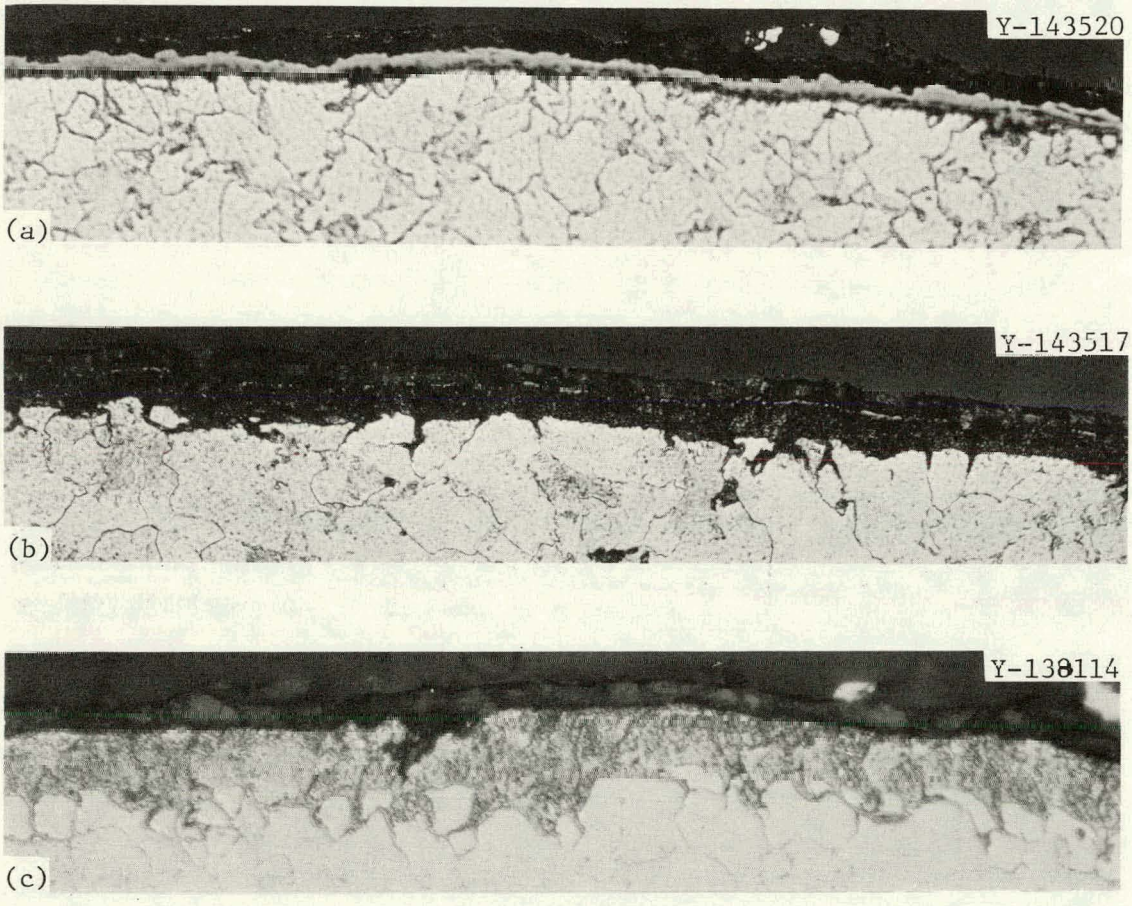

Fig. 18. Edge of Cross Section of Gage Section of 2 1/4 Cr-1 Mo Steel Specimen Exposed in Simulated HTGR-Helium Environment at Three Different Temperatures. (a) Test 15374 (Heat 36202), exposed at 482°C (900°F) for 13,509 hr. (b) Test 15046 (Heat X-6216), exposed at 538°C (1000°F) for 14,957 hr. (c) Test 15023 (Heat X-6216), exposed at 593°C (1100°F) for 9660 hr. 500×.

Small cross-sectional samples were cut from the gage section of several of the 2 1/4 Cr-1 Mo steel creep specimens and analyzed for carbon. One sample was also analyzed for hydrogen, oxygen, and nitrogen. The results are shown in Table 8 together with the analyses of the unexposed material. The specimen that was exposed for 13,509 hr at 482°C (900°F) showed virtually no change in the carbon content (the very slight increase observed may be due to the limited accuracy of analysis), whereas the steel was decarburized when the exposure temperature was 538°C (1000°F) or above. The rate of decarburization increased with increasing temperature. The increased content of oxygen probably came from the thin oxide layer that formed during the test.

The data obtained to date on the corrosion specimens of 2 1/4 Cr-1 Mo steel exposed in an unstressed condition inside the HTGR-helium environmental creep furnaces are shown in Table 9. Those specimens that are listed more than once in the table have been exposed for more than one creep test period. They were reweighed before they were remounted for a new creep test. Although the data base is sparse and exposure times are short, the results were consistent in that all specimens exposed at 593°C (1100°F) gained weight, and all specimens exposed at 649°C (1200°F) lost weight.

Table 8. Analysis of 2 1/4 Cr-1 Mo Steel Specimens Tested in Simulated HTGR-Helium Environment

Test	Heat	Test Conditions			Results of Analysis, ppm			
		Temperature		Time (hr)	C	H	O	N
		(°C)	(°F)					
	36202	Isothermally annealed			1420			
15374	36202	482	900	13509	1460			
	X-6216	Isothermally annealed			1216	9	40	125
15046	X-6216	538	1000	14957	1050			
15023	X-6216	593	1100	9660	729	7	547	127
17864	X-6216	649	1200	513	860			

Table 9. Results of Weight Gain Measurements on 2 1/4 Cr-1 Mo Steel (Heat 20017) Plate Specimens Exposed in Simulated HTGR-Helium Environments

Specimen	Temperature (°C)	Temperature (°F)	Exposure Time (hr)	Weight Gain (mg)	Weight Gain (g/m^2)
KB 3	593	1100	90	0.7	1.0
KB 4	593	1100	90	0.7	1.0
KB 5	593	1100	328	0.6	0.8
KB 3	593	1100	418	1.3	1.8
KB 1	593	1100	793	1.2	1.6
KB 2	593	1100	793	1.2	1.6
KB 6	649	1200	288	−0.1	−0.1
KB 7	649	1200	288	−0.2	−0.3
KB 13	649	1200	361	−0.5	−0.7
KB 10	649	1200	513	−0.2	−0.3
KB 7	649	1200	801	−0.5	−0.7
KB 7	649	1200	1162	−1.5	−2.0

Some Corrosion Observations on Hastelloy X Exposed to HTGR Helium

The same kinds of examinations (metallographic, chemical analysis for carbon, and weight change) of 2 1/4 Cr-1 Mo steel were also made of the Hastelloy X alloy.

By examining the surface at a cross section of the shoulder (where the stress was one-fourth that at the gage section) one can assess the corrosion behavior of this material in the HTGR environment. The oxide formed on the surface of Hastelloy X exposed to HTGR helium differs only slightly from that formed in air at 704°C (1300°F). The differences are more distinct at 760°C (1400°F), and even more pronounced at 816°C (1500°F). As shown in Figs. 19 through 21, there was no difference in specimens exposed to the HTGR helium at the three temperatures, but it is evident that attack in air increases with increasing temperature.

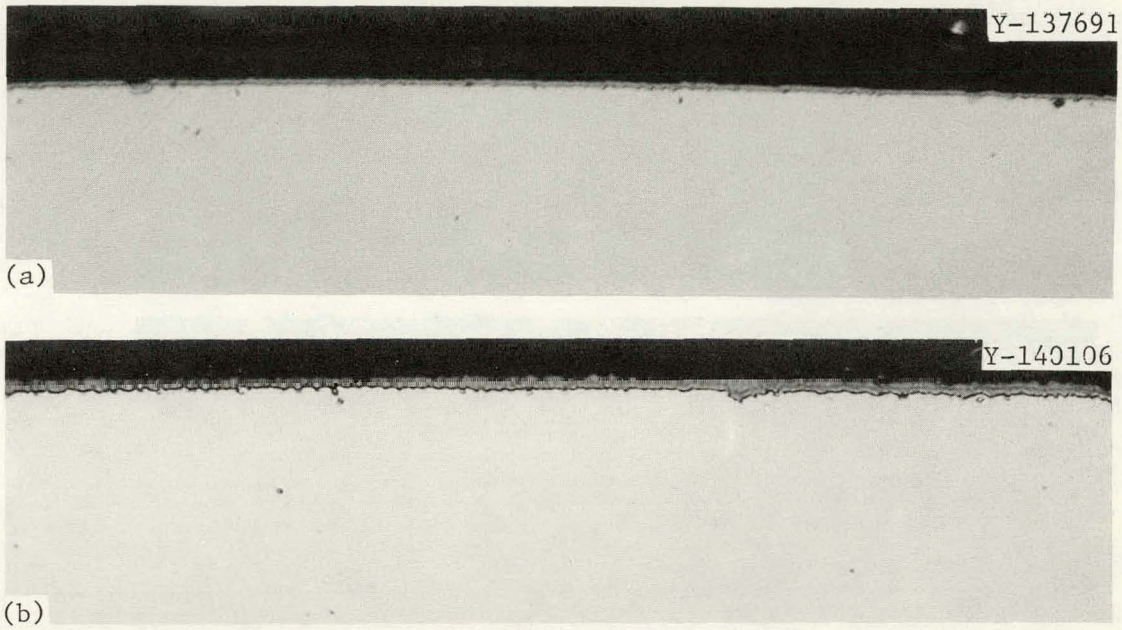

Fig. 19. Edge of Cross Section of the Shoulder of Hastelloy X Creep Specimens (Heat 2600-3-4936). (a) Test 15792, HTGR-helium-exposed for 4588 hr at 704°C (1300°F). (b) Test 16268, air-exposed for 4504 hr at 704°C (1300°F). 500×.

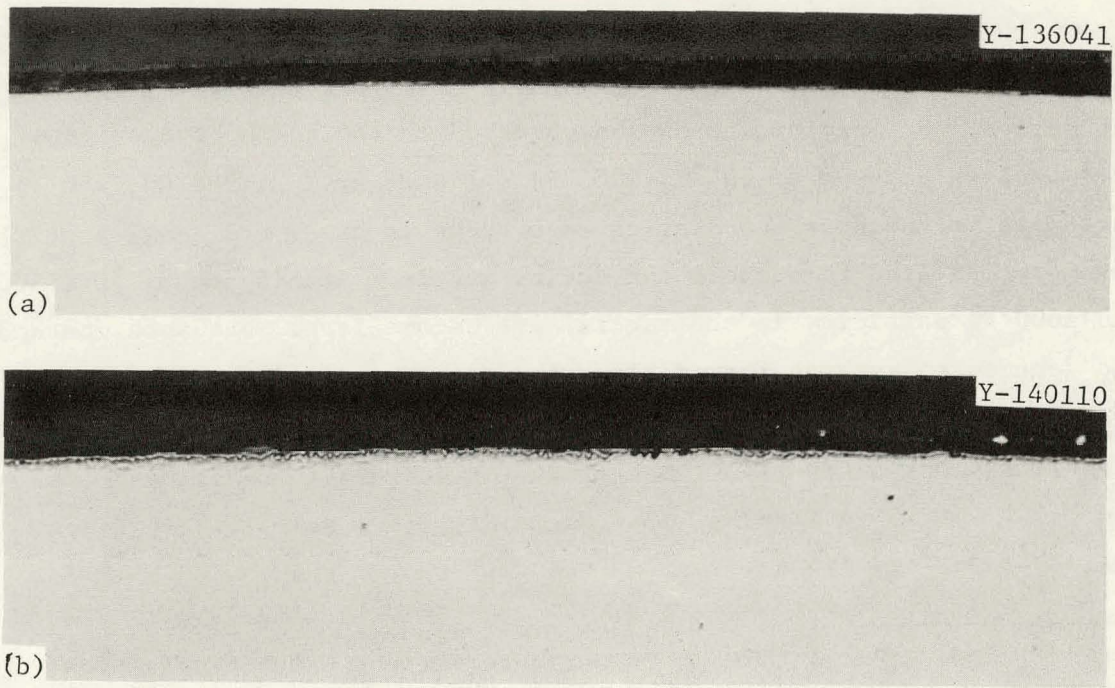

Fig. 20. Edge of Cross Section of the Shoulder of Hastelloy X Creep Specimens (Heat 2600-3-4936). (a) Test 16125, HTGR-helium exposed for 305 hr at 760°C (1400°F). (b) Test 17330, air exposed for 297 hr at 760°C (1400°F). 500×.

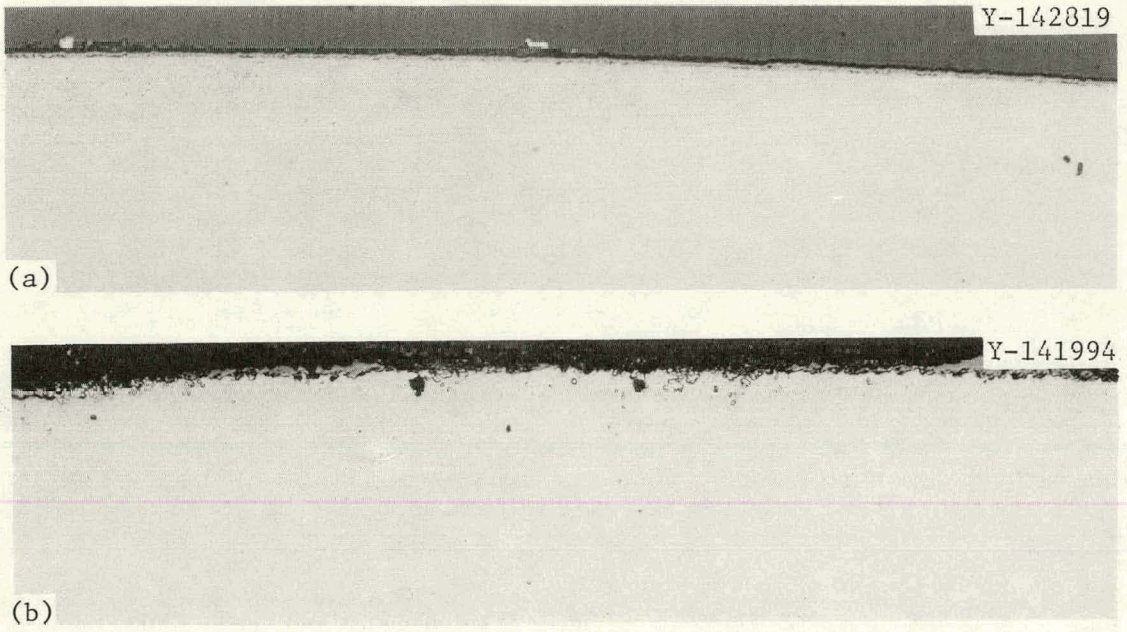

Fig. 21. Edge of Cross Section of Shoulder of Hastelloy X Creep Specimens (Heat 2600-3-4936). (a) Test 17332, HTGR-helium-exposed for 2790 hr at 816°C (1500°F). (b) Test 17375, air-exposed for 1905 hr at 816°C (1500°F). 500×.

The changes in microstructure of Hastelloy X as a function of the exposure temperature are shown in Fig. 22. The as-received material (solution annealed) shows only a slight precipitation in the grain boundaries, but precipitate can be observed in the grain boundaries of the specimen exposed at 704°C (1300°F) for 4588 hr. At 760°C (1400°F) particles in the grain boundaries have grown in size, and small particles have precipitated throughout the entire matrix. At 816 and 871°C (1500 and 1600°F) particles in the martix have become large, but more sparse, and denuded zones have formed along the grain boundaries. According to Jablonski[16] the precipitates are mainly carbides of the M_6C and $M_{23}C_6$ types. The $M_{23}C_6$ type is primarily of the composition $Cr_{21}(Mo,W)_2C_6$, and the M_6C types range from $M_{2.48}C = Mo_{0.91}Ni_{0.90}Cr_{0.50}Fe_{0.17}C$ to $M_{13.25}C = Mo_{6.34}Ni_{5.73}Cr_{0.69}Fe_{0.49}C$.

---

[16]D. A. Jablonski, "High Temperature Fatigue Crack Propagation Behavior of Two Super Alloys," Master's Thesis, Massachusetts Institute of Technology, January 1976.

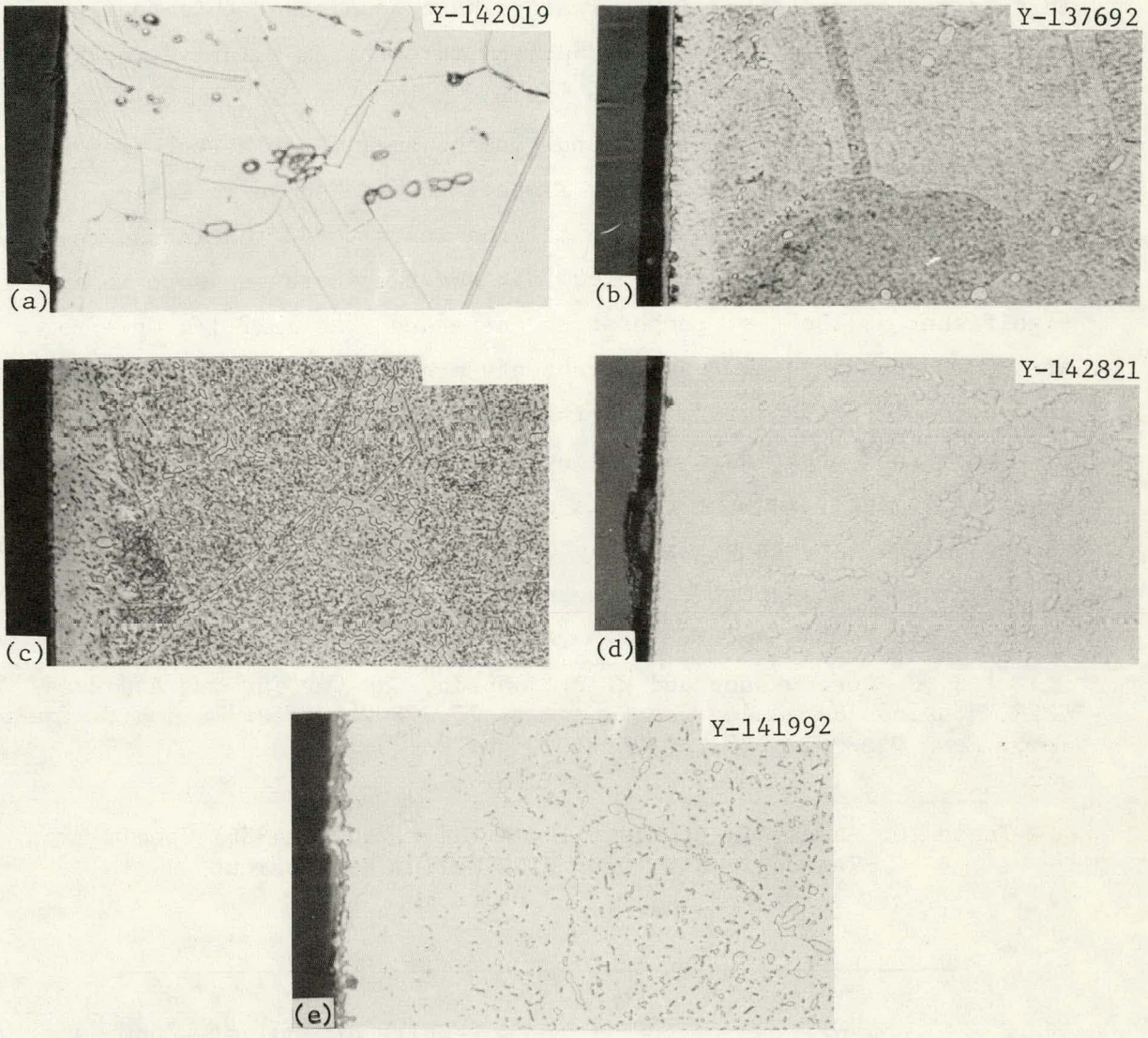

Fig. 22. Edge of Cross Section of Shoulder of Hastelloy X Creep Specimens (Heat 2600-3-4936) Exposed in Simulated HTGR-Helium Environment at Different Temperatures, Showing the Change in the Microstructure. (a) As-received (solution annealed). (b) Test 15792, exposed at 704°C (1300°F) for 4588 hr. (c) Test 16490, exposed at 760°C (1400°F) for 2690 hr. (d) Test 17332 exposed at 816°C (1500°F) for 2790 hr. (e) Test 16126, exposed at 871°C (1600°F) for 6527 hr. 500×.

Another microstructural feature of the specimens in Fig. 22 is the subsurface zone below the surface layer. Precipitation is very light in this region and other investigators have found that this region is rich in nickel and iron but depleted in chromium relative to the nominal composition of the alloy.[17]

The results of the carbon analyses on small samples cut from the gage section of tested Hastelloy X specimens are shown in Table 10. Carbon contents increased during all the tests conducted in the temperature range of 649–871°C (1200–1600°F), and the increases were more significant as the test temperature increased. As in 2 1/4 Cr-1 Mo steel, increases in the oxygen contents are likely the result of the thin oxide layer that formed during the test.

Only four unstressed Hastelloy X weight-gain specimens have been examined to date, and the results are shown in Table 11. The specimens gained weight at both 649 and 816°C (1200 and 1500°F), and the amount of weight gain was greater at the higher temperature.

---

[17]S. N. Rosenwasser and W. R. Johnson, *Gas Turbine and Advanced HTGR Materials Screening Test Program, 10,000-Hour Results and Semiannu. Prog. Rep. Mar. 31, 1977*, GA-A14407, pp. 2–125.

Table 10. Analysis of Hastelloy X (Heat 2600-3-4936) Specimens Tested in Simulated HTGR-Helium Environment

Test	Test Conditions			Results of Analysis, ppm			
	Temperature		Time (hr)	C	H	O	N
	(°C)	(°F)					
	as received			792	11	21	545
15772	649	1200	6466	830			
15792	704	1300	4588	820			
16490	760	1400	2690	880			
17332	816	1500	2790	1010			
16126	871	1600	6527	1334	8	555	545

Table 11. Results of Weight Gain Measurements on Hastelloy X (Heat 2600-3-4936) Plate Specimens Exposed in Simulated HTGR-Helium Environment

Specimen	Temperature		Exposure Time	Weight Gain	
	(°C)	(°F)	(hr)	(mg)	(g/m^2)
X 1	649	1200	4793	1.6	2.2
X 2	649	1200	4793	1.5	2.0
X 3	816	1500	2790	2.6	3.5
X 4	816	1500	2790	2.4	3.3

SUMMARY AND CONCLUSIONS

Environmental equipment has been developed for high-temperature creep testing of structural materials in simulated HTGR helium. The creep test program of 2 1/4 Cr-1 Mo steel and Hastelloy X is in an early stage, and very few test data have been obtained for times longer than 6000 hr. Therefore, all conclusions based on these creep data should be considered as preliminary.

1. Tensile tests performed on isothermally annealed 2 1/4 Cr-1 Mo steel showed minima in the strength and ductility in the temperature range of 260—370°C. Strength values were consistent with those in the *Nuclear Systems Materials Handbook*.

2. A minimum in the short-term tensile ductility of Hastelloy X, which is typical for nickel-base high-temperature alloys, fell in the temperature range 480—705°C.

3. Comparisons of creep behavior and creep-rupture data of 2 1/4 Cr-1 Mo steel in HTGR helium and air show no significant difference in rupture life and time to tertiary creep, whereas the minimum creep rate was lower for the HTGR-helium tests than for the air tests.

4. Stress-rupture data for Hastelloy X in simulated HTGR helium showed no significant difference from those obtained in air, whereas the minimum creep rate was lower in HTGR helium than in air in the range of 649—871°C. The lower the stress, the larger was the difference between creep rates in helium and air.

5. Creep curves of Hastelloy X obtained in HTGR helium and air under three different test conditions were compared. They showed no difference as long as the test temperature was 760°C or below. At 816°C the minimum creep rate was more than twice as high for the air test as for the HTGR-helium test.

6. Micrographs of cross sections of tested 2 1/4 Cr-1 Mo steel specimens showed that the corrosion rate at 593°C in HTGR helium decreases with increasing time and that the depth of attack reached 20 μm in 9660 hr. The corrosion rate in air was much higher.

7. Small samples from the gage section of tested 2 1/4 Cr-1 Mo steel specimens exposed at 482°C showed no change in carbon content, whereas the steel specimens decarburized when the exposure temperature was 538°C or above. Decarburization increased with increasing temperature.

8. Unstressed weight-gain specimens of 2 1/4 Cr-1 Mo steel exposed to HTGR-helium at 593°C gained weight, and the ones exposed at 649°C lost weight.

9. There was only a slight difference in oxide formation at 704°C on the surface of Hastelloy X exposed to HTGR helium compared with air. The corrosion rate in air was slightly higher at 760°C and much higher at 816°C.

10. Hastelloy X exposed at 704°C (1300°F) showed some precipitation in grain boundaries. At 816 and 871°C large particles precipitated throughout the matrix and denuded zones formed along the grain boundaries.

11. The carbon content increased in Hastelloy X specimens tested in HTGR helium. The increase was greater at higher test temperatures.

12. All specimens of unstressed Hastelloy X exposed to HTGR helium at 649 and 816°C gained weight. As temperature increased, weight gain became larger.

ACKNOWLEDGMENTS

The authors gratefully acknowledge E. B. Patton, Jr., E. Bolling, B. McNabb, and C. W. Houck for carrying out the experimental work; J. C. Griess and H. E. McCoy for reviewing, Ray Ihrig for editing, and Gail Golliher for preparation of the manuscript.

THIS PAGE

WAS INTENTIONALLY

LEFT BLANK

ORNL/TM-6001
Distribution
Category UC-77

INTERNAL DISTRIBUTION

1–2. Central Research Library
3. Document Reference Section
4–13. Laboratory Records Department
14. Laboratory Records, ORNL RC
15. ORNL Patent Office
16. R. J. Beaver
17. M. K. Booker
18–27. C. R. Brinkman
28. J. P. Callahan
29. D. A. Canonico
30. J. H. Coobs
31. J. M. Corum
32–34. W. R. Corwin
35. F. L. Culler
36. J. E. Cunningham
37. J. H. DeVan
38–47. J. R. DiStefano
48. R. G. Donnelly
49. G. G. Fee
50. B. L. Greenstreet
51. J. C. Griess, Jr.
52. J. P. Hammond
53. W. O. Harms
54–56. M. R. Hill
60. F. J. Homan
61. H. Inouye
62. P. R. Kasten
63. J. F. King
64. R. T. King
65. R. L. Klueh
66. K. C. Liu
67. A. L. Lotts
68. A. P. Malinauskas
69. H. E. McCoy
70. C. J. McHargue
71. R. K. Nanstad
72. P. Patriarca
73. S. Peterson
74. H. Postma
75. P. L. Rittenhouse
76. T. K. Roche
77. J. P. Sanders
78. J. L. Scott
79. V. K. Sikka
80. G. M. Slaughter
81–88. J. P. Strizak
89. D. B. Trauger
90. J. R. Weir, Jr.
91. G. D. Whitman
92. R. W. Balluffi (Consultant)
93. P. M. Brister (Consultant)
94. W. R. Hibbard, Jr. (Consultant)
95. Hayne Palmour III (Consultant)
96. J. W. Prados (Consultant)
97. N. E. Promisel (Consultant)
98. D. F. Stein (Consultant)

EXTERNAL DISTRIBUTION

99–100. ERDA DIVISION OF REACTOR NUCLEAR RESEARCH AND APPLICATIONS, Washington, DC 20545

Director

101. ERDA IDAHO OPERATIONS OFFICE, P. O. Box 2108, Idaho Falls, ID 83401

Barry Smith

102. ERDA OFFICE PROGRAM MANAGEMENT, RESEARCH AND SPACE PROGRAMS, P.O. Box 81325, San Diego, CA 92138

J. B. Radcliffe

EXTERNAL DISTRIBUTION (Continued)

103. ERDA SAN FRANCISCO OPERATIONS OFFICE, 1333 Broadway, Wells Fargo Building, Oakland, CA 94612

Manager

104–106. ERDA DIVISION OF WASTE MANAGEMENT, PRODUCTION AND PROCESSING, Washington, DC 20545

Chief, Technology Branch
Chief, Projects Branch
Chief, Industrial Programs Branch

107–109. ERDA OAK RIDGE OPERATIONS DIVISION, P.O. Box E, Oak Ridge, TN 37830

Director, Research and Technical Support Division
Director, Reactor Division
F. E. Dearing, Reactor Division

110–286. ERDA TECHNICAL INFORMATION CENTER, P.O. Box 62, Oak Ridge, TN 37830

For distribution as shown in TID-4500 Distribution Category, UC-77 (Gas-Cooled Reactor Technology).

287–294. ERDA Exchange Agreements with Germany and Dragon Project

☆ U.S. GOVERNMENT PRINTING OFFICE: 1977-748-189/276